scientific reports

Check for updates

OPEN

EEG oscillations reveal neuroplastic changes in pain processing associated with long-term meditation

Juliana Yordanova[1]✉, Valentina Nicolardi[2], Peter Malinowski[3], Luca Simione[4], Salvatore M. Aglioti[2,5], Antonino Raffone[2,6] & Vasil Kolev[1]

The experience of pain is a combined product of bottom-up and top-down influences mediated by attentional and emotional factors. Meditation states and traits are characterized by enhanced attention/emotion regulation and expanded self-awareness that can be expected to modify pain processing. The main objective of the present study was to explore the effects of long-term meditation on neural mechanisms of pain processing. EEG pain-related oscillations (PROs) were analysed in highly experienced practitioners and novices during a non-meditative resting state with respect to (a) local frequency-specific and temporal synchronizing characteristics to reflect mainly bottom-up mechanisms, (b) spatial synchronizing patterns to reflect the neural communication of noxious information, (c) pre-stimulus oscillations to reflect top-down mechanisms during pain expectancy, and (d) the P3b component of the pain-related potential to compare the emotional/cognitive reappraisal of pain events by expert and novice meditators. Main results demonstrated that in experienced (long-term) meditators as compared to non-experienced (short-term) meditators (1) the temporal and spatial synchronizations of multispectral (from theta-alpha to gamma) PROs were substantially suppressed at primary and secondary somatosensory regions contra-lateral to pain stimulation within 200 ms after noxious stimulus; (2) pre-stimulus alpha activity was significantly increased at the same regions, which predicted the suppressed synchronization of PROs in long-term meditators; (3) the decrease of the P3b component was non-significant. These novel observations provide evidence that even when subjected to pain outside of meditation, experienced meditators exhibit a pro-active top-down inhibition of somatosensory areas resulting in suppressed processing and communication of sensory information at early stages of painful input. The emotional/cognitive appraisal of pain is reduced but remains preserved revealing a capacity of experienced meditators to dissociate pro-active and reactive top-down processes during pain control.

Keywords Pain, Meditation, EEG, Pain-related oscillations

Pain signifies a life-threatening condition. The subjective experience of pain is therefore accompanied by strong emotional reflections of unpleasantness, attention redirection to the noxious event, and behavioural reactions of avoidance and self-protection[1–6]. Moreover, pain perception is critically modulated by ongoing emotional, motivational and attentional brain states mediated by contextual variables[7–9]. Accordingly, pain is conceptualized as an integrative process whereby the unique pain experience is a combined product of bottom-up and top-down influences[9–11].

In line with this complexity, neuroimaging studies in humans and animals show that the experience of pain is accompanied by a co-existing involvement of a variety of cortical and subcortical structures[2,6,8,12–16], with most consistent activations established for the anterior cingulate cortex (ACC), the insular cortex (IC), primary and secondary somatosensory cortices (S1, S2), thalamus, and associative cortices[2,4,16–22].

[1]Institute of Neurobiology, Bulgarian Academy of Sciences, Acad. G. Bonchev Str., Bl. 23, 1113 Sofia, Bulgaria. [2]Department of Psychology, Sapienza University of Rome, Rome, Italy. [3]School of Psychology, Research Centre for Brain and Behaviour, Liverpool John Moores University (LJMU), Liverpool, UK. [4]Institute of Cognitive Sciences and Technologies, CNR, Rome, Italy. [5]Neuroscience and Society Lab, Istituto Italiano Di Tecnologia, Rome, Italy. [6]School of Buddhist Studies, Philosophy and Comparative Religions, Nalanda University, Rajgir, India. ✉email: j.yordanova@inb.bas.bg

Top-down influences on pain can depend on transient, state-dependent, and trait-dependent factors. Transient *contextual factors* related to expectancy, attention and salience can change subjective pain perception from moment to moment depending on whether attention is actively directed to or away from pain stimulus or divided between noxious and innocuous stimuli or between different sources of painful input (e.g.,[23–27]). Tonic *fluctuations of brain states* induced by e.g., trust, worry, fear, or placebo represent another important class of top-down influences on pain[9,28,29]. Finally, trait-dependent individual dispositions supported by an *inherent organization* of neural networks are critical for the top-down modulations of pain in normal and pathological (e.g., chronic pain) conditions[30–36].

In this perspective, it is notable that the most distinctive features of meditation states and traits encompass enhanced attention and emotion regulation and expanded self-awareness[37–43]. Long-term meditation practice has been associated with neuroplasticity marked by structural and functional changes in large-scale executive networks[44–47]. Practitioners with established meditation expertise have manifested intrinsic changes in the functional connectivity of fronto-parietal and medial frontal networks involved in executive control (attention and performance monitoring)[48–50]. Extensive mindfulness practice also leads to changes in the functional connectivity of the default mode and salience networks associated with enhanced self-awareness and attention/emotion regulation[49,51]. The neural correlates of meditation states and traits also comprise brain networks that are specifically implicated in pain experience—thalamus, IC and ACC[37,52–54].

In accordance with these findings, meditation has been reported to suppress subjective pain[55–59]. Based on subjective pain evaluations, it is now generally acknowledged that meditation positively influences noxious event perception by modulating primarily the emotional and attention-related components of pain[55,57,59–63]. This is confirmed by various studies demonstrating significant improvements in affective pain relative to sensory pain in meditation[64].

Two neurophysiological models have been suggested to account for altered pain experience in mediation[64,65]. The first one is based on observations that long-term meditation training is accompanied by greater activation in somatosensory regions and deactivation of appraisal-related regions such as ACC and ventro-medial prefrontal cortex[66,67]. This dissociation in activation between appraisal-related and sensory areas suggests that expert meditators are able to separate the sensory experience of pain from the corresponding evaluation[68,69]. That is, they *do* sense noxious stimuli as fairly painful but do not evaluate the unpleasantness/affect that traditionally accompanies painful experiences, thus removing the need for top-down inhibitory control[65–67,70]. Referring to Buddhist meditation traditions where pain perception is considered, this mechanism might be described as blocking the "second arrow of pain" [58].

The second model, suggested by Zeidan et al.[71,72], involves a downregulation of ascending nociceptive signals in the thalamus. This downregulation is achieved through effortful cognitive processes mediated by executive attention that results in lower signaling in relevant somatosensory areas[71,73]. This mechanism is suggested to transform ascending nociceptive information from painful to innocuous, thus avoiding the need for further extensive cognitive/affective reappraisal[64,65]. Within the Buddhist tradition, this mechanism might be described as blocking the "first arrow of pain"[58].

These models are essentially derived from neuroimaging studies such as fMRI, in which the fine temporal dynamics of underlying processes cannot be precisely assessed. A fine-grained temporal resolution of brain signals can, however, be provided by electroencephalographic (EEG) and magnetoencephalographic (MEG) signals. EEG studies of pain processing have shown that evoked pain potentials and patterns of neural responses are generated in different regions, at different time scales and in different frequency bands—theta, alpha, beta, and gamma[10,18,24,27,74–88]. It is now increasingly recognized that the sensory and contextual components of pain may be differentially associated with the frequency, timing and synchronizing properties of neural pain-related oscillations[10]. Specifically, evoked pain-related potentials (PRPs) and local oscillatory alpha-to-gamma responses to noxious stimuli are more sensitive to bottom-up (e.g., physical intensity) than to top-down processes (e.g. expectation, preparatory attention)[77,85,87,89]. In contrast, top-down influences are reflected by ongoing oscillatory activity from alpha and beta frequency ranges preceding noxious event delivery[90–93]. Top-down influences (expectations) also have been linked to pain-related spatial synchronization of alpha and gamma oscillatory networks after painful stimulation[94]. In addition, the late parietal P3b component of event-related potentials that reflects the amount of attention allocated to cognitive stimulus evaluation[95] is considered an index of involuntary attentional shift to nociceptive events[96–98].

The main objective of the present study was to shed further light on the neural mechanisms of pain processing of meditators by analysing pain-related oscillations (PROs). Toward this end, EEG responses to noxious stimuli were recorded and analysed in highly experienced practitioners and novices during a non-meditative resting state[47,50,58]. PROs were analysed with respect to (a) local frequency-specific and temporal synchronizing characteristics to reveal mainly bottom-up mechanisms and activations of somatosensory and associative cortical regions, (b) spatial synchronizing patterns of pain-related oscillatory networks to reveal the communication of noxious information, (c) pre-stimulus oscillations to reveal top-down mechanisms during pain expectancy, and (d) the P3b PRP component to compare the emotional/cognitive reappraisal of pain events by expert and novice meditators.

We hypothesized that neural responses to pain would be altered in long-term practitioners outside of meditation during a non-meditative rest condition due to neuroplastic changes in executive and pain-related brain networks. We also expected that pain-related oscillations would provide new evidence about the effects of long-term meditation on bottom-up and top-down mechanisms of pain regulation, which would help to further test and substantiate the existing models.

Methods

In the present study we analysed a selected data sets from a large project investigating a unique sample of long-term meditators. Subjective pain measures from the pain experiment have been reported by Nicolardi et al. [58], in which EEG and neural pain responses were not considered. We used records of spontaneous EEG from the same sample (reported in Yordanova et al. [47,50]) as a no-pain control condition, but the present new analyses are not reported elsewhere.

Participants

A total of 35 participants were studied. They were divided into two groups – long-term meditators (LTM) and control short-term meditators (STM). The group of LTM included twenty monastics from the Theravada Buddhist tradition (3 females; mean age = 44.6 ± 10.9, mean number of years in monastery = 18 ± 12.7). The participants were monks and nuns residing at Amaravati Buddhist Monastery, in Southern England, and at Santacittarama Monastery, in Central Italy. Despite the different geographic locations, practices at both monasteries are aligned with the Thai Forest Theravada Buddhist tradition, which is now established, widely acknowledged and influential in the West. In this tradition, practitioners typically practice two hours per day with the monastery community, with a regular intensification of practice during retreats. According to inclusion criteria, participants were required to have practiced focused attention meditation (FAM), open monitoring meditation (OMM), and loving-kindness meditation (LKM) forms in a balanced way, often in integrated sessions, including silent meditation retreats (3 months per year). As suggested by the abbots of the monasteries, monastics were included who had an average of 100 h of practice per month during monastic life, with a balance of meditation facets. In the present study, meditation expertise was measured in hours taking into account both practice in the monastic tradition and practice before monastic life. The lifetime duration of meditation practice of the LTM was estimated as a mean of 19,358 h (SE = 3164), range 900–50,600 h. The group of STM included 15 short-term meditation practitioners (6 females, mean age = 44.8 ± 8.2) who each had a total of less than 250 h of meditation experience. All participants were right-handed healthy volunteers, without a history of neurologic, psychiatric, chronic somatic, or other problems. Although LTM data were acquired at different places, the main criteria for sample selection emphasized on the type and duration of meditation expertise, which was controlled across places to enable comparisons with STM. The study was approved by the dedicated Research Ethics Committee at Sapienza University of Rome, Italy. All participants gave informed consent before participation according to the Declaration of Helsinki.

Tasks and procedures

Neural responses to painful electrical pulses generated by a monophasic constant current stimulator (STIM140, H.T.L. srl, Amaro, UD, Italy) were recorded. Stimuli were delivered through two surface electrodes (diameter 6 mm, Ag–Cl, Electro-Cap International, Inc. Eaton, Ohio) placed 5 mm from each other. The stimulation site was on the dorsal digital branch of the radial nerve, on the medial surface of the back of the left hand. The intensity range allowed by the instrument was between 2 and 50 mA.

As depicted in Fig. 1, the whole experimental procedure consisted of three phases: (1) determination of the absolute pain threshold, (2) stimulus intensity calibration, (3) task and stimulation blocks. During the first phase, the absolute pain threshold of each participant was identified as the minimum intensity of a stimulus perceived as painful. The threshold was determined by the ascending and descending method of limits[99,100]. During the second calibration phase, supra-threshold electric stimuli were delivered with a staircase procedure until the participant associated the same stimulus intensity with a moderate pain sensation in 50 ± 10% of probes. The threshold and calibration phases allowed the selection of a moderately intense stimulus for each participant, to be used during the next stimulation blocks. The third experimental phase consisted of a series of painful stimuli delivered as single events during conditions which the participants were instructed to maintain in succession: a non-meditative resting state (REST) condition, and 3 meditation conditions. In the present study, only the REST condition was analyzed. Participants were instructed to remain in a non-meditative resting state with eyes closed while pain stimuli were delivered. The explicit instruction for the REST condition was: Rest in a non-meditative relaxed state, without falling in sleep, while allowing any spontaneous thoughts and feelings to arise and unfold in the field of experience. There were 3 REST blocks, each including 10 trials leading to a total of 30 trials. The effects on neural pain processing of specific meditation states vs. REST will be presented in a separate study.

The trial duration was approximately 10 s (9 to 13 s). The painful stimulus (electrical stimulus with 50 ms duration) was delivered randomly 4.5 to 8.5 s after beginning of the trial. One and half second after stimulus delivery, participants were asked to rate (scale 1–100) three dimensions of subjective experience related to the nociceptive stimulation: pain, aversion, and identification [58].

EEG recording and pre-processing

EEG was recorded by a mobile wireless system (Cognionics; https://www.cognionics.net/mobile-128) using an electrode cap with 64 active Ag/AgCl electrodes located in accordance with the extended international 10/10 system and referenced to linked mastoids. Electrode impedances were kept below 10 kOhm and EEG signals were collected at a sampling rate of 500 Hz (resampled off-line to 250 Hz for data analysis).

EEG analysis was performed with Brain Vision Analyzer ver. 2.2.2 (Brain Products GmbH, Gilching, Germany). EEG traces were visually inspected for gross ocular and other artefacts at 64 channels. Contaminated trials were discarded along with EEG records exceeding ± 100 μV. Bad channels were interpolated using topographic interpolation[101]. Slight horizontal and vertical eye movements preserved in the accepted trials were corrected by means of independent component analysis (ICA)[102]. After artefact rejection, the mean number of artefact-free trials used for analysis of each subject was 27 (SD = 2.3, range 24–29, consistent with standards).

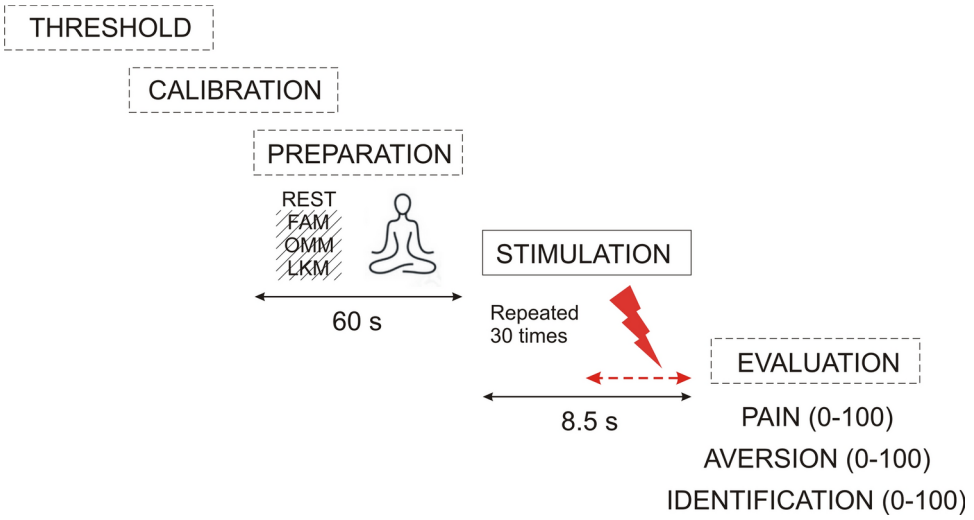

Fig. 1. Experimental procedure and trial details. After the measurement of the subjective pain threshold (THRESHOLD phase), participants underwent the CALIBRATION phase to find a moderate value to be used during the task. The task included a brief interval (1 min) to engage in the mind-set of non-meditative REST, or meditative focused attention (FAM), open monitoring (OMM), and loving kindness (LKM) meditation type (PREPARATION). The engagement interval was followed by STIMULATION—a transient painful electrical stimulus delivered with a random inter-stimulus interval within the second half of an 8.5-s-long period (red-dotted line). Each stimulus was followed by three visual scales for ratings (from 0 to 100) of pain, aversion and identification experiences (EVALUATION). Note: For the present study only the REST condition was used.

Current source density

Current source density (CSD) transform of the signals was performed off-line to achieve a reference-free evaluation and control for volume conduction (see, e.g.,[101,103] for details). The spherical Laplace operator is applied to the potential distribution on the surface of the head. This procedure provides excellent estimates of the bioelectric activity of the cortical surface when applied with dense electrode arrays (48–256 electrodes, 64 in the present study)[103]. All EEG epochs (spontaneous and pain-related responses) were re-referenced and analysed after a CSD transform of the signals.

Analysis of pain-related EEG responses

In the present study, pain EEG responses were analysed in the time- and time–frequency domains. Averaged time-domain PRPs were computed to extract the P3b component reflecting cognitive pain evaluation. Time–frequency decomposition was applied to target specifically the temporal and spatial synchronization features of PROs after stimulus[104–107] and to examine ongoing oscillatory networks by exploring total power in the pre-stimulus periods. The power of averaged PROs was used for preliminary analyses.

Time-domain analysis was performed by averaging 1.5-s long artefact-free pain-related EEG epochs, including 0.5 s before and 1 s after electric stimulus. P3b was identified as the maximal positive peak with centro-parietal/parietal distribution within 300–500 ms after stimulus[95]. Peak amplitude and latency of P3b were measured against a baseline of 300 ms before stimulus.

Time–frequency (TF) analysis of pain-related potentials was performed by means of a continuous wavelet transform (CWT) with Morlet wavelets as basis functions[108]. Complex Morlet wavelets *W(t,f)* can be generated in the time domain for different frequencies, *f*, according to the equation:

$$W\left(t,f\right)=A\exp\left(-t^2/2\sigma_t^2\right)\exp\left(2i\pi ft\right) \quad (1)$$

where t is time, $A=\left(\sigma_t\sqrt{\pi}\right)^{-1/2}$, σ_t is the wavelet duration, and $i=\sqrt{-1}$ is the imaginary unit.

To identify precisely low- and high-frequency oscillatory responses to pain, two types of epochs were analysed in the TF domain:

(1) For slow-frequency PROs from the delta, theta, and alpha frequency bands, EEG epochs were 1.5 s long, including 0.5 s before and 1 s after the electric stimulus.

(2) For fast-frequency PROs from beta and gamma frequency bands, EEG epochs were 0.85 s long, with 0.25 s before and 0.6 s after stimulus.

WT parameters also were adjusted to slow- and fast-frequency PROs:

(1) For analysis of slow-frequency PROs, wavelet family was characterized by a ratio of $f_0/\sigma_f=4$, where f_0 is the central frequency and σ_f is the width of the Gaussian shape in the frequency domain. This f_0/σ_f ratio was oriented to slower phase-locked components as providing a decrease in the decay of the shape of the Morlet wavelet[109]. For different f_0, time and frequency resolutions can be calculated as $2\sigma_t$ and $2\sigma_f$, respectively, with σ_t and σ_f being

related by the equation $\sigma_t = 1/(2\pi\sigma_f)$. The analysis was performed in the frequency range 0.5–25 Hz with a central frequency at 0.6 Hz intervals.

(2) To adjust parameters to fast-frequency PROs, the second WT decomposition was performed in the frequency range 15–50 Hz with a central frequency at 1.75 Hz intervals, and a wavelet family characterized by the ratio of $f_0/\sigma_f = 10$, oriented to the higher frequencies accordingly. These two types of TF decompositions were applied to averaged and single-trial PRPs.

Phase-locked power of PROs

Different methods of evaluation are required to assess the power of phase-locked and non-phase-locked activity[74]. Here, to compute phase-locked activity, the wavelet transform was applied to the averaged PRPs, which enabled the extraction of phase-locked power (PLP)[109].

Total power of PROs

Total power (TOTP) comprises both the phase-locked and non-phase-locked activity. To include the non-phase-locked portion of the signal, single trials were first transformed to the TF domain and then averaged. For each trial, the time-varying power in a given frequency band was calculated, which was obtained by squaring the absolute value of the convolution of the signal with the complex wavelet. In the present study, TOTP was used for analysis of pre-stimulus activity. Frequency-relevant TOTP measures were extracted in alpha, beta and gamma frequency ranges (Fig. 6) and analysed. For statistical evaluation, TF power was log10-transformed.

Temporal synchronization of PROs: Phase-locking factor

The temporal phase synchronization across trials was analysed by means of the phase-locking factor (PLF, e.g.,[110,111]). The PLF provides a measure of synchronization of oscillatory activity independently of the signal's amplitude. The values of PLF yield a number between 0 and 1 determining the degree of between-sweep phase-locking, where 1 indicates perfect phase alignment across trials and values close to 0 reflect the highest phase variability. PLFs were computed for different TF scales at each time-point for each electrode and subject.

Spatial synchronization of PROs: Phase-locking value

Following methodological recommendations[112], phase-based connectivity was assessed using phase-locking values (PLVs). This approach (a) is recommended for hypothesis-driven vs. exploratory analyses, as targeted here, (b) is robust to time dynamics, time lag, frequency mismatches, and frequency non-stationarities, and (c) is robust to increased variance in phase stability.

PLVs between electrode channels measure the extent to which oscillation phase angle differences between electrodes are consistent over trials at each time/frequency point. As a measure of spatial synchronization, PLVs were computed for different TF scales at each time-point t and trial j according to the equation:

$$PLV_{k,l} = \left| \frac{1}{N} \sum_{j=1}^{N} e^{i\left(\rho_{j,k}(t,f_0) - \rho_{j,l}(t,f_0)\right)} \right| \quad (2)$$

where N is the number of single sweeps, k and l are indices for the pair of electrodes to be compared, and ρ is the instantaneous phase of the signal. $PLV_{k,l}$ results in real values between one (constant phase difference) and zero (random phase difference). PLV was computed for each pair of electrodes, resulting in a total of 630 pairs (after excluding the edge electrodes prone to signal distortion due to the lack of neighbour electrodes, and reducing the number of electrodes to 35) for each subject.

To identify regions with maximal connectivity during PRPs, the mean of all pairs connected with each single electrode was computed for each electrode. Following this procedure, a quantifier 'regional PLV' (R-PLV) was established. For R-PLV computation the selected 35 electrodes were used (F5, F3, Fz, F4, F6, FC5, FC3, FCz, FC4, FC6, C5, C3, Cz, C4, C6, CP5, CP3, CPz, CP4, CP6, P7, P5, P3, Pz, P4, P6, P8, PO7, PO3, POz, PO4, PO8, O1, Oz, and O2). Time–frequency plots of R-PLV also were computed for each subject and electrode.

Control analysis of spontaneous EEG.

As detailed in Yordanova et al.[47], EEG was recorded with eyes closed for 5–6 min in no pain conditions REST, FAM, OMM, and LKM using the same recording setup and pre-processing. The experiment was conducted in a quiet, dimly lit room suitable for meditation and recording EEG. Using ICA and CSD EEG was pre-processed as described in 2.3 and 2.4. All analyses were carried out with CSD-transformed data from 50 electrodes. EEG recordings were segmented in equal-sized epochs of 4.096-s duration with 1.024-s overlap. The average number of epochs for each participant was 70 (± 20). After the Hanning window with a duration of 20% from the total epoch length applied to all epochs, fast Fourier transform (FFT) was computed, yielding the representation of complex values with a frequency resolution of 0.244 Hz (1/4.096 s).

Parameters and selection of ROIs

Selection of synchronized time–frequency pain-related components

Figure 2 demonstrates time–frequency plots of PLP for slow and fast PROs of STM and LTM during REST. Inspection of TF plots in STM reveals that in the slow frequency band (left panel A), two main components were temporally synchronized by pain stimulus – theta-alpha (5–10 Hz) and delta (1.5–4 Hz). In the fast frequency bands (right panel B), three distinct TF components were evident – beta (16–25 Hz), slow gamma (gamma-1, 30–35 Hz), and fast gamma (gamma-2, 38–42 Hz). Inspection of TF plots in LTM demonstrates that these TF components of pain potentials were strongly reduced in LTM. In addition, it is shown that the maximal expression of frequency-specific PROs occurred with different timing after pain stimulation: within 500 ms

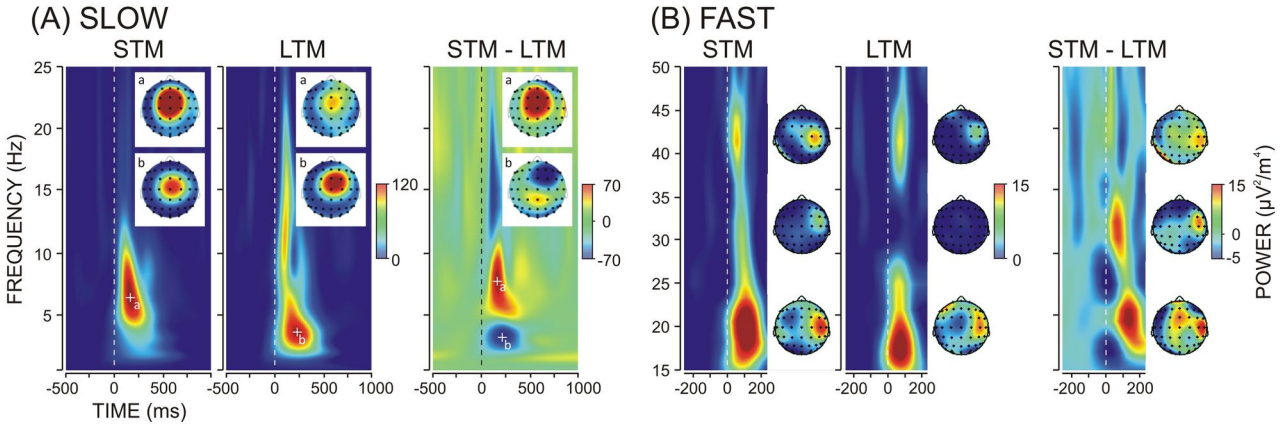

Fig. 2. Time–frequency (TF) plots and topography distribution maps of the phase-locked power for (A) slow-frequency and (B) fast-frequency pain-related oscillations of short-term (STM) and long-term (LTM) meditators during resting state. Difference TF plots and difference topography maps (STM-LTM) are depicted for each TF component. The TF plots are presented for C4 electrode. For slow TF components in (A), 'a' refers to theta-alpha mainly expressed in STM and 'b' refers to delta TF component mainly expressed in LTM. Stimulus occurrence at 0 ms.

time window for delta (group mean across all electrodes 200 ± 80 ms), within 250 ms for theta-alpha (group mean 128 ± 20 ms), within 200 ms for beta (group mean 110 ± 15 ms), and within 150 ms for gamma-1 (group mean 80 ± 10 ms) and gamma-2 (group mean 50 ± 10 ms). Figure 2 also demonstrates the different topographic distributions of frequency-specific components. Specifically, an anterior midline dominance is observed for delta and theta-alpha, whereas a focused localization at central/postcentral contralateral (right-hemisphere) electrodes is demonstrated for beta, gamma-1, and gamma-2 TF components.

TF Components and Measurements

Based on all these observations, 5 relevant TF components were selected for analysis: delta with central frequency f_0 = 3.12 Hz (1.5 – 4.5 Hz), theta-alpha with f_0 = 7.5 Hz (4.7 – 10.7 Hz), beta with f_0 = 18.14 Hz (15.8 – 22.9 Hz), gamma-1 with f_0 = 32.1 Hz (30.8 – 35.9 Hz), and gamma-2 with f_0 = 43.5 Hz (38.8 – 42.9 Hz).

PLF and R-PLV were measured as the maximal value within defined epochs after stimulus for each frequency band, subject, and electrode as follows: delta (within 40–500 ms), theta-alpha (within 20–250 ms), beta (within 10–150 ms), gamma-1 (within 10–150 ms), gamma-2 (10–100 ms). The measures were baseline corrected by subtracting the mean value of a baseline of −300/−50 ms for slow and −200/−50 ms for fast frequency TF components.

Pre-stimulus activity was measured by computing the mean value of TOTP for theta-alpha and alpha (f_0 = 7.5 and 10.1 Hz) layers within −450/−50 ms, beta (−250/−50 ms), and gamma-1/gamma-2 (−220/−40 ms) frequency bands. These three frequency ranges were chosen for analysis of pre-stimulus activity as being distinctively present before stimulus (Fig. 6).

Thus, in *the time–frequency domain*, the final parameters used for analysis were:

(1) PLF reflecting the stability of temporal phase synchronization of TF components in relation to pain stimulus,

(2) R-PLV reflecting the strength of functional connectedness of maximally synchronized regions during pain processing, and.

(3) TOTP reflecting pre-stimulus activity,

(4) For control analyses, spectral power of the spontaneous EEG was measured in alpha, beta and gamma frequency-bands and analysed after being log-transformed.

In *the time domain*, amplitude and latency of time-domain P3b component were analyzed to reflect the amount of cognitive pain stimulus appraisal.

Selection of Regions of Interest (ROIs)

TF analyses were performed for sets of electrodes covering three regions of interest (ROIs): (1) contralateral primary somatosensory cortex (S1), (2) contralateral secondary somatosensory cortex including the insular cortex (S2-IC), and (3) frontal medial cortex including the ACC and supplementary motor areas (FM). These three ROIs were selected basing on (1) theoretical accounts according to which S1, S2, IC, and ACC are the major regions with relevant cortical projections involved in pain processing[2,16]; (2) observations from current data on phase-locked pain-related activity (Fig. 2); (3) previous detailed topographic analysis of phase-locked PROs evoked by similar nociceptive stimulation[74]; and (4) previous approaches for analysis of synchronized pain-related oscillations and spatial connections[89,94]. Following the correspondence of electrode positions of the 10/10 system to these areas[113,114], S1 included Cz, C4, CPz, CP4[89], S2-IC included C6, CP6, and P6, and FM included Fz and FCz electrodes. The Fz/FCz electrodes were chosen as having been proved to capture the joint activation of supplementary motor areas and ACC.

Statistical analysis

The statistical analysis tested the hypothesis that PROs differ between experienced and novice meditators in the REST condition. Analyses were performed for each ROI and each frequency-specific PLF/R-PLV/TOTP measure. A repeated-measures ANOVA was used with the between-subjects variable Group (STM vs. LTM) and the within-subjects variable Electrode (specific for each ROI). Analyses of P3b latency and amplitude were performed at centro-parietal electrodes (CP3, CPz, CP4, detailed in the Results). One-way ANOVA was employed to evaluate the effects of Group on pain threshold and measures of subjective pain evaluation (pain perception, aversion, and identification). In control and complementary analyses, to explore the associations between PRO synchronization and sensitivity to pain as well as the associations between PRO synchronization and pre-stimulus activity, multiple regression stepwise analyses were applied as detailed in the Results. Pearson correlation coefficients also were computed to assess the associations between the examined PRO and pre-stimulus activity, and between different objective and subjective parameters. For factors with more than two levels, the Greenhouse–Geisser correction was applied to the degrees of freedom (*df*). Original *df*, corrected *p*-values, and partial eta squared are reported, along with mean group values ± standard error (SE) whenever relevant. To control for multiple testing effects, FDR correction was applied[115]. For all analyses, only significant statistical outcomes are presented in detail in the results.

Results

Subjective pain indices

Pain thresholds tended to be lower in STM than LTM (Group, $F(1/34) = 3.6$, $p = 0.06$, $\eta^2 = 0.106$). None of the parameters reflecting subjective pain (subjective pain intensity, aversion, and identification) differed significantly between the two groups during REST (Group, $p > 0.2$).

Effects of long-term meditation on PRO synchronization

Figure 3 depicts TF plots of PLF in the groups of STM and LTM during REST. It confirms the presence of slow and fast TF components as observed in averaged potentials (PLPs) and demonstrates that the expression of these components results from a prominent local phase-synchronization with pain stimulus.

Figure 4 presents time–frequency plots of R-PLV during REST and shows that pain processing is supported by synchronized frequency-specific oscillatory networks in the same frequency ranges. Similar to the temporal phase-synchronization, delta and theta-alpha oscillations manifested maximal spatial synchronization at the midline with slight lateralization in the right hemisphere, whereas beta, gamma-1, and gamma-2 oscillations manifested a focused localization of the maximal spatial synchronization at contra-lateral (right-hemisphere) electrodes.

The statistical effects of the Group factor on the synchronization of PRO parameters during REST at three ROIs (S1, S2-IC, and FM) are presented in Table 1 and graphically illustrated in Fig. 5. Consistent with the observations from difference maps in Fig. 3, PLFs of theta-alpha, beta, gamma-1, and gamma-2 PROs were significantly larger in STM than LTM at S1 and S2-IC (Table 1, Fig. 5). Confirming the topography-specific differences between groups observed in Fig. 4, the spatial synchronization (R-PLV) was significantly stronger in STM than LTM at S1 for beta, and at S2-IC for theta-alpha and gamma-2 PROs (Table 1, Fig. 5). No significant group effects were revealed at the FM ROI for the local temporal or spatial synchronization (Table 1).

These results show that during pain processing, the temporal and spatial synchronization of multi-spectral pain-related oscillations is substantially suppressed in long-term meditators at primary and secondary somatosensory cortical areas contra-lateral to the side of pain stimulus.

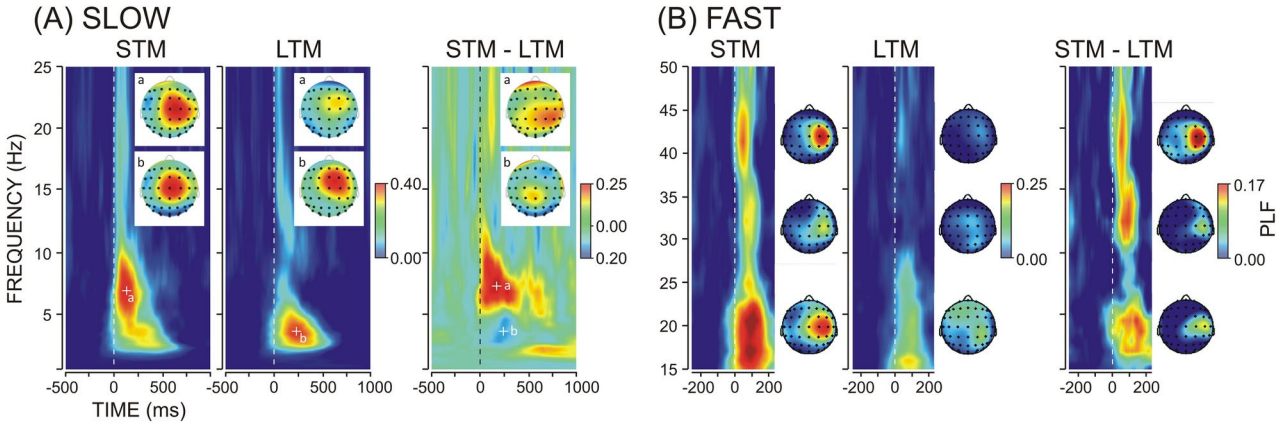

Fig. 3. Time–frequency plots and topography distribution maps of the phase-locking factor (PLF) for (**A**) slow-frequency and (**B**) fast-frequency pain-related oscillations in short-term (STM) and long-term meditators (LTM) during resting state. Difference TF plots and difference topography maps (STM-LTM) are depicted for each TF component. The TF plots are presented for the C4 electrode. For slow TF components in (A), 'a' refers to theta-alpha and 'b' refers to delta TF component. Stimulus occurrence at 0 ms.

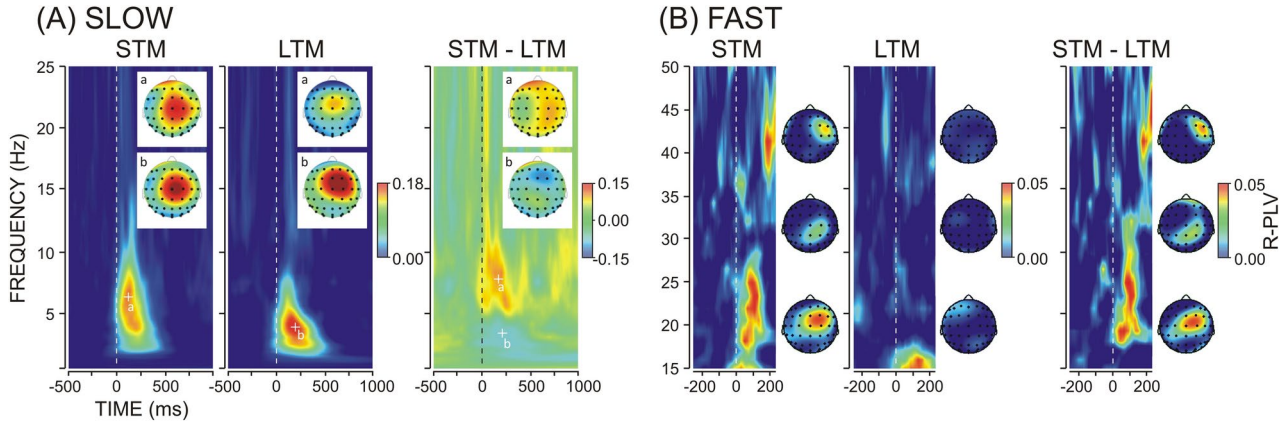

Fig. 4. Time–frequency (TF) plots and topography distribution maps of the regional phase-locking value (R-PLV) for (**A**) slow-frequency and (**B**) fast-frequency pain-related oscillations of short-term (STM) and long-term meditators (LTM) during resting state. Difference TF plots and difference topography maps (STM-LTM) are depicted for each TF component. The TF plots are presented for the C4 electrode. For slow TF components in (A), 'a' refers to theta-alpha and 'b' refers to delta TF component. Stimulus occurrence at 0 ms.

Variable	S1			S2-IC			FM		
Group ***(df = 1/33)***	***F***	***p***	η^2	***F***	***P***	η^2	***F***	***p***	η^2
(a) PLF									
Delta	ns			ns			ns		
Theta-Alpha	8.15	0.008	0.203	6.22	0.018	0.163	ns		
Beta	6.92	0.01	0.178	ns			ns		
Gamma-1	6.72	0.001	0.179	6.55	0.015	0.170	ns		
Gamma-2	11.9	0.001	0.270	ns			ns		
(b) R-PLV									
Delta	ns			ns			ns		
Theta-Alpha	3.9	0.05	0.121	4.55	0.04	0.125	ns		
Beta	3.8	0.05	0.109	ns			ns		
Gamma-1	ns			ns			ns		
Gamma-2	ns			7.86	0.008	0.197	ns		
(c) Pre-stimulus									
Alpha	6.22	0.02	0.163	8.69	0.006	0.214	ns		
Beta	ns			ns			ns		
Gamma	5.79	0.02	0.153	4.42	0.05	0.116	ns		

Table 1. Statistical results from testing the effects of Group (STM vs. LTM) during REST on (a) phase-locking factor (PLF), (b) regional phase-locking value (R-PLV) of PROs, and (c) pre-stimulus power of oscillations from different frequency bands (delta, theta-alpha, beta, gamma-1, and gamma-2) at three ROIs (S1, S2-IC, FM).

Effects of long-term meditation on pre-stimulus activity during REST

Pre-stimulus activity in the slow and fast frequency bands is illustrated in Fig. 6. Statistical effects of the Group factor on pre-stimulus alpha, beta and gamma activity during REST at three ROIs (S1, S2-IC, and FM) are presented in Table 1. It is demonstrated that pre-stimulus alpha and gamma activities were significantly higher in LTM than STM at S1 and S2-IC, whereas beta activity did not differ reliably between the two groups. At the FM ROI, no Group effects were yielded.

Effects of long-term meditation on P3b PRP component

To confirm P3b identity, the topographic distribution of peak P3 amplitude was analysed in a Region (5 levels corresponding to fronto-central, central, centro-parietal, and parietal regions) x Laterality (5 levels corresponding to left ventral, left dorsal, midline, right dorsal and right ventral electrodes) ANOVA. As expected, P3b PRP component was maximal at the midline (Laterality, $F(4/132) = 8.6$, $p < 0.001$, $\eta^2 = 0.212$) and at centro-parietal electrodes (Region, $F(4/132) = 4.1$, $p = 0.02$, $\eta^2 = 0.118$) – Fig. 7 (right). At centro-parietal electrodes P3b was larger in STM than LTM but this difference did not reach significance ($F(1/33) = 3.7$, $p = 0.06$, $\eta^2 = 0.104$). Peak P3b latency did not differ between STM (group mean = 350 ± 7.4 ms) and LTM (group mean = 347 ± 6.6 ms).

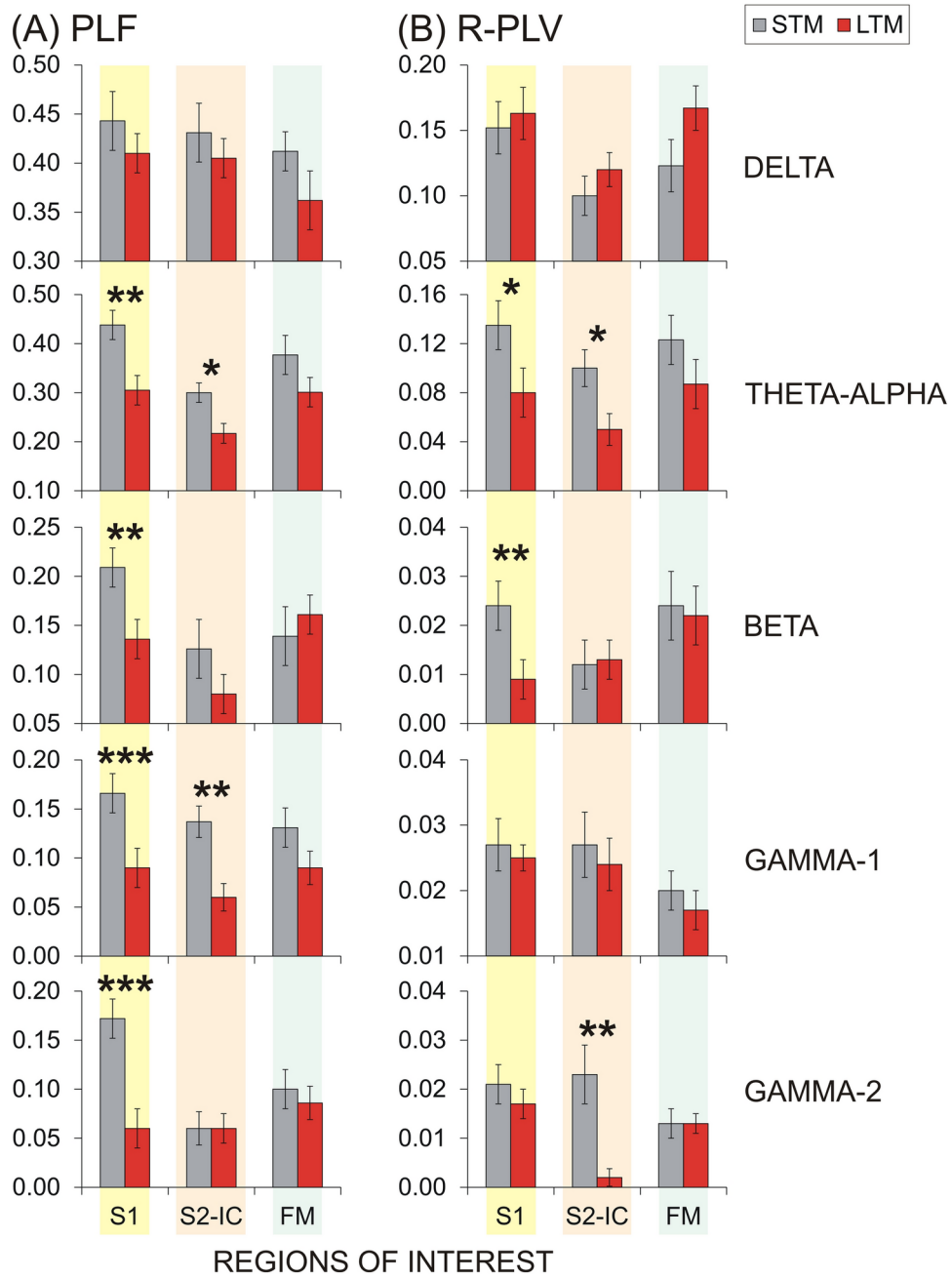

Fig. 5. Group means ± SE of (**A**) phase-locking factor and (**B**) regional PLV of delta, theta-alpha, beta, gamma-1, and gamma-2 PROs in short-term (STM) and long-term meditators (LTM) at three ROIs (S1, S2-IC, and FM). Statistical between-group differences are indicated by asterisks (* $p < 0.05$; ** $p < 0.01$; *** $p < 0.001$).

Control analyses

It is well documented that alpha and fast-frequency activities are enhanced in long-term meditators[39,116]. Two control analyses were carried out to test if the pre-stimulus alpha and gamma activities of LTM are specifically increased at contra-lateral S1 and S2-IC during the pain condition. The first control analysis aimed to check if these rhythms were larger in the present sample of LTM than STM in resting state no-pain condition, or if the enhancement in LTM was only linked to the pain stimulation. The second control analysis assessed the lateral asymmetry of these rhythms in no-pain and pain conditions to see if pain stimulation is accompanied by a specific topographic reallocation of ongoing rhythms related to preparation for pain processing in the hemisphere contra-lateral to stimulation[84,90,91,117].

(1) Control analysis 1: Spontaneous alpha and gamma activities were analysed during resting state where no pain stimulation was applied. As in the pain condition, they were compared between STM and LTM at S1 and S2-IC, i.e., at those ROIs where these pre-stimulus activities were enhanced in LTM before pain stimulation. A significant Group effect was found for the spontaneous alpha activity at S1 ($F(1/33) = 12.5$, $p = 0.001$, $\eta^2 = 0.075$)

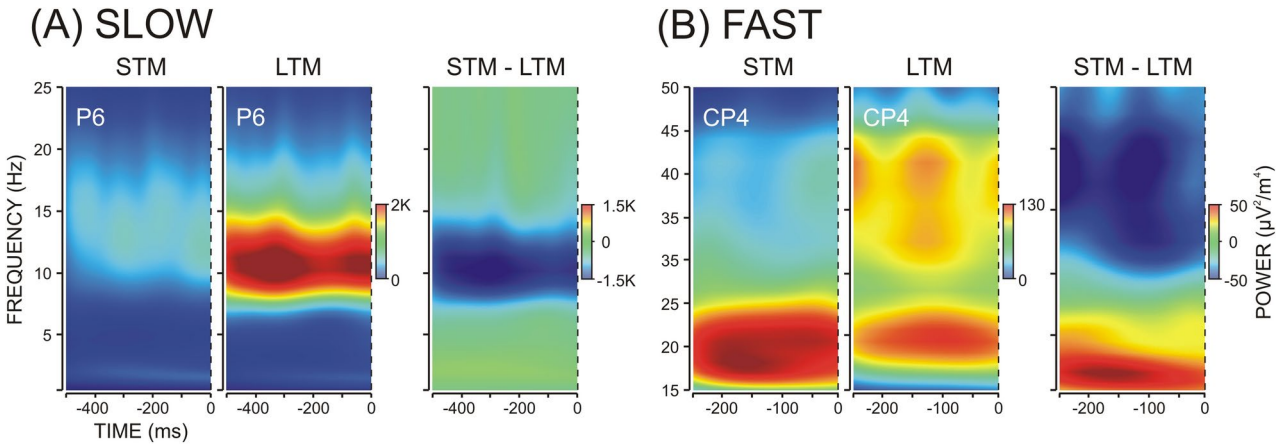

Fig. 6. Time–frequency (TF) plots of the pre-stimulus total power for (**A**) slow-frequency and (**B**) fast-frequency bands of short-term (STM) and long-term meditators (LTM) at representative electrodes P6 and CP4. Difference TF plots (STM-LTM) are presented on the right. Stimulus occurrence at 0 ms.

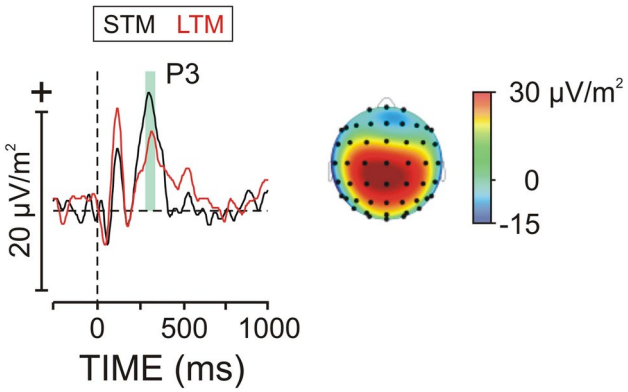

Fig. 7. Pain-related potentials in the time domain in short-term (STM) and long-term meditators (LTM) at Pz. The map depicts P3 peak topographic distribution. Stimulus occurrence at 0 ms.

and S2-IC ($F(1/33) = 10.2$, $p = 0.002$, $\eta^2 = 0.062$), reflecting larger spontaneous alpha in the group of LTM. Spontaneous fast-frequency activity did not differ significantly between the groups at S1 ($p > 0.3$) but it was enhanced in LTM at S2-IC ($F(1/33) = 5.8$, $p = 0.02$, $\eta^2 = 0.048$). These observations imply that the pre-stimulus enhancement of alpha and gamma oscillations in LTM during pain may reflect a background neuroplastic state of alpha and gamma networks in highly experienced meditators rather than a specialized role in controlling the brain state before noxious events.

(2) Control analysis 2: To explore further the possible specific involvement of pre-stimulus oscillations in the pain condition, pre-stimulus alpha and gamma powers were computed at ipsi-lateral S1 and S2-IC and compared with contra-lateral values in each group. Likewise, the lateral asymmetry of alpha and gamma power was analysed during resting state where no pain stimuli were delivered. Repeated-measures ANOVAs with a between-factor Group (STM vs. LTM) and Laterality (right vs. left) were used. Analyses in the alpha band revealed that in STM, no laterality (right vs. left) difference existed at either S1 or S2-IC during no-pain (Laterality, $F(1/14) = 1.9$, $p = 0.2$, $\eta^2 = 0.04$; $F(1/14) = 1.42$, $p = 0.2$, $\eta^2 = 0.04$) and pain conditions (Laterality, $F(1/14) = 1.37$, $p = 0.3$, $\eta^2 = 0.09$; $F(1/14) = 0.72$, $p = 0.4$, $\eta^2 = 0.05$). In contrast, while in the group of LTM, alpha activity at ipsi- and contra-lateral S1 and S2-IC also did not differ during the no-pain condition (Laterality, $F(1/19) = 1.8$, $p = 0.2$, $\eta^2 = 0.02$; $F(1/19) = 2.1$, $p = 0.2$, $\eta^2 = 0.018$), a significant contra-lateral > ipsi-lateral (right > left) effect was yielded in the pain stimulation condition at both S1 (Laterality, $F(1/19) = 13.9$, $p = 0.002$, $\eta^2 = 0.43$) and S2-IC (Laterality, $F(1/19) = 6.4$, $p = 0.02$, $\eta^2 = 0.26$) regions. No lateralized differences were found for gamma activity in any condition (no pain or pain) and group, implying that the enhancement of pre-stimulus gamma oscillations may not specifically subserve brain states involved in the preparation for pain processing.

Asymmetry index of alpha activity was additionally computed as the normalized difference between right-hemisphere and left-hemisphere measures and statistically analysed for S1, S2-IC and frontal regions (F3 and F4) using ANOVA with a between factor Group (STM vs. LTM) and Condition (NO PAIN vs. PAIN). The results of these analyses are illustrated in Fig. 8. They confirmed the observed right > left asymmetry for S1 and S2-IC

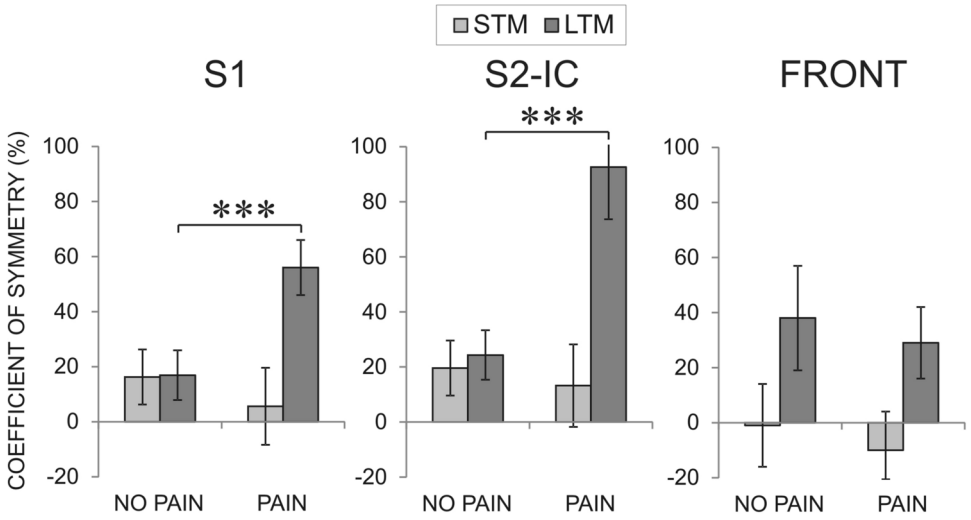

Fig. 8. Group mean values ± SE of the normalized asymmetry index (%) in NO PAIN (derived from spontaneous EEG) and PAIN conditions at S1, S2-IC and FM regions in short-term (STM) and long-term meditators (LTM). Significant simple effects of Condition were observed in the group of meditators for S1 and S2-IC, *** $p < 0.001$. S1, primary somatosensory cortex; S2-IC, contralateral secondary somatosensory cortex including the insular cortex; FRONT, frontal cortex.

only in LTM only during the pain condition, thus further emphasizing the specificity of alpha involvement at S1 and S2-IC before pain stimulation in LTM (Fig. 8).

Together, these observations demonstrate that pre-stimulus alpha activity is specifically enhanced at contralateral primary and secondary somatosensory regions before painful stimulation only in experienced meditators.

Complementary analyses

Relationships between PRO synchronizations and pain processing

According to our main observations, PRO synchronizations at S1/S2-IC during REST were suppressed in the group of LTM, whereas subjective pain measures (pain intensity, aversion, identification) did not differ between the groups. Yet, sensitivity to noxious stimulus intensity (as reflected by threshold) also differentiated STM from LTM. To test if the PRO synchronization might relate to pain processing, the relationships with the threshold were analysed. In several multiple regression stepwise analyses, the threshold was included as a dependent variable and synchronization measures (PLF or R-PLV) at S1/S2-IC electrodes were included as predictors ($n = 7$ for each analysis). This design was chosen because each frequency-specific PRO, PLF, or R-PLV measures at S1/S2-IC electrodes were positively inter-correlated ($r = 0.315 \div 0.518$, $p = 0.01 \div 0.001$). By accounting for these inter-correlations the multiple stepwise regression models would extract the most relevant predictions at specific electrodes. Because separate analyses were performed for each frequency band and each measure (PLF and R-PLV), FDR correction of p was implemented setting it to 0.01. The extracted statistically relevant PLF/R-PLV predictors for each TF component are illustrated in Fig. 9. The statistical results of the corresponding regression models are presented in Table 2. Opposite to intuitive negative relationships implied by between-group effects, the regression analyses demonstrated that (1) threshold was positively associated with theta-alpha, beta, gamma-1, and gamma-2 PLF at S1 electrodes, and (2) threshold was positively associated with theta-alpha, beta, gamma-1, and gamma-2 R-PLV at both S1 and S2-IC electrodes (Fig. 9). The observed positive associations imply that the high threshold is accompanied by strong temporal and spatial synchronizations of PROs at primary and secondary somatosensory areas.

The same analyses were performed for pre-stimulus alpha, beta and gamma activity to explore if pre-stimulus activations may directly modulate sensitivity to pain stimulus intensity as implied by previous research[91]. In contrast to post-stimulus PRO synchronizations, no such associations were found.

Relationships between PRO synchronization and pre-stimulus activity

It is acknowledged that enhanced pre-stimulus activity can deteriorate the temporal phase-locking of stimulus-related oscillations[118]. Hence, the reduction of the temporal and spatial synchronizations of PROs in LTM may result from the increased pre-stimulus activity in alpha and/or gamma band in this group. To test this hypothesis, similar multiple regression stepwise analyses were carried out. In separate analyses, each PLF and R-PLV measure at each of the S1 and S2-IC electrodes was the dependent variable and pre-stimulus alpha or gamma measures at the S1/S2-IC electrodes ($n = 7$) were the predictors. Again, this design was chosen because for each frequency band (alpha and gamma), the pre-stimulus activity at S1/S2-IC electrodes was highly positively inter-correlated ($r = 0.326 \div 0.950$, $p = 0.01 \div 0.001$). It was found that (1) Suppressed theta-alpha and gamma-2 PLF and R-PLV at S1/S2-IC were predicted by enhanced pre-stimulus alpha power at S1 electrodes ($R^2 = 0.164 \div 0.180$; $F(1/33) = 6.27 \div 19.05$, $p = 0.01 \div 0.001$; $Beta = -0.365 \div -0.425$, $t = -2.2 \div -2.6$, $p = 0.01$), (2) Suppressed beta PLF and R-PLV at S2 were predicted by enhanced pre-stimulus alpha at S2 ($R^2 = 0.214 \div 0.290$; $F(1/33) = 6.47 \div 9.3$,

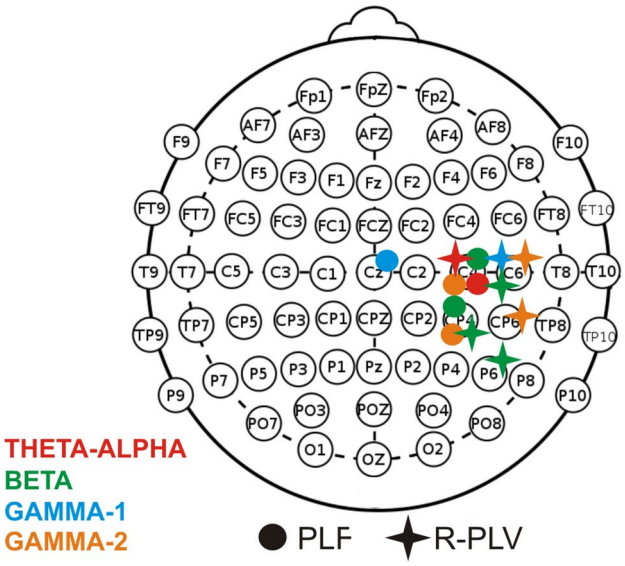

Fig. 9. Position of electrodes at which PLF (circle) and R-PLV (asterisk) measures were extracted as predictors of threshold in multiple stepwise regression analyses.

Independent variables	R^2	*F*	*P*	*B*	*Beta*	*t*	*p*
(a) PLF							
Theta-Alpha	0.513	29.5	< 0.001	27.4	0.716	5.4	< 0.001
Beta	0.404	19.2	< 0.001	41.3	0.636	4.4	< 0.001
Gamma-1	0.302	12.1	0.002	54.8	0.549	3.5	0.002
Gamma-2	0.262	9.9	0.004	80.8	0.512	3.2	0.003
(b) R-PLV							
Theta-Alpha	0.381	17.2	< 0.001	63.2	0.617	4.9	< 0.001
Beta	0.490	26.9	< 0.001	31.3	0.700	5.2	< 0.001
Gamma-1	0.232	8.5	0.007	22.2	0.482	2.9	0.006
Gamma-2	0.332	6.7	0.004	23.8	0.465	2.7	0.01

Table 2. Statistical results from multiple stepwise regression models with dependent variable threshold (T) and independent predictors synchronization measures (PLF, R-PLV) of theta-alpha, beta, gamma-1, and gamma-2 pain-related oscillations at S1 and S2-IC electrodes, df = 1/33.

$p = 0.01 \div 0.005$; Beta $= -0.364 \div -0.512$, $t = -2.4 \div -3.8$, $p = 0.01$), (3) Suppressed gamma-1 PLF and PLV at S1/S2-IC were predicted by high pre-stimulus alpha power at S2-IC ($R^2 = 0.145 \div 0.314$; $F(1/33) = 5.47 \div 14.71$, $p = 0.02 \div 0.001$; Beta $= -0.382 \div -0.561$, $t = -2.4 \div -4.8$, $p = 0.02 \div 0.001$), and (4) With exception of beta PLF and gamma-1/gamma-2 R-PLV, suppressed PLF and R-PLV of the other frequency-specific PROs were predicted by increased pre-stimulus gamma power but the significance of the models was marginal ($p = 0.05 \div 0.04$).

These observations reveal that the strength of pain-related temporal and spatial synchronizations of multispectral PROs at both S1 and S2-IC areas is critically modulated by pre-stimulus alpha activity.

Discussion

The present study was designed to explore the effects of long-term meditation on the neural mechanisms of pain processing as reflected by pain-related oscillations and potentials. Because extensive meditation practice cultivates enhanced awareness and attention/emotion regulation accompanied by neuroplastic reorganization of neural networks, it was expected that PROs would differ between experienced and novice meditators also during a non-meditative resting state condition.

Confirming this hypothesis, main results demonstrate that in experienced meditators as compared to short-term meditators (1) the temporal and spatial synchronizations of multispectral pain oscillations were substantially suppressed at primary and secondary somatosensory regions contra-lateral to pain stimulation; (2) alpha activity preceding pain stimulus was significantly increased and re-allocated to the same contra-lateral regions; (3) the increase in pre-stimulus alpha activity predicted the suppressed synchronization of pain-related oscillations in experienced meditators; (4) the suppression of post-stimulus synchronization was associated with reduced sensitivity to pain stimulus intensity; and (5) the centro-parietal P3b PRP component was smaller in experienced than novice meditators though this effect was not reliable. Likewise, the PROs at associative fronto-

medial regions did not differ between the two groups. As detailed below, these observations indicate that long-term meditation alters the neurophysiological mechanisms of bottom-up and top-down pain processing.

In the present study, noxious electric stimulation elicited complex EEG pain-related oscillations including delta, theta-alpha, beta, gamma-1 and gamma-2 components. This observation is consistent with reports demonstrating the compound multispectral characteristics of pain EEG responses (rev.[10]). So far, phase relationships of PROs have not been addressed systematically in pain research. Previous studies have analysed the components of local time-domain potentials (e.g.,[18,24,80,87,89,119,120]. However, time-domain components are modulated by both the temporal synchronization and magnitude of EEG responses[104–107]; thus, the information about underlying synchronization processes is confounded. Previous pain research also has explored oscillatory power modulations (even-related synchronization/desynchronization ERS/ERD) in longer (e.g., 1 s) epochs after a noxious event (rev.[121]). Yet, phase relationships are crucial for understanding the neural functions of cortical oscillations involved in pain perception and behaviour[121]. Indeed, an early study by Babiloni et al.[74] has demonstrated that the processing of pain events is critically reflected by the temporal phase synchronization of evoked oscillations from multiple frequencies (from theta to gamma) in the very early epochs (up to 100 ms) after noxious input. In particular, a significantly stronger synchronization is elicited by noxious as compared to innocuous stimuli and the scalp distribution of phase-locked oscillations is different from that of the non-phase-locked ones[74]. Later studies have confirmed the specific relevance of early (0–200 ms) phase-locked beta and gamma PROs generated in the sensorimotor cortex for integrative pain perception[27,79,122,123].

The present analyses contribute to further clarifying the synchronization properties of neuroelectric pain responses and their functional involvement. Specifically, they reveal that the temporal and spatial phase-locking of overlapped multi-spectral oscillations represents an important early stage of pain processing. Moreover, in line with Babiloni et al.[74], they demonstrate that slow- and fast-frequency PROs have different topographic distributions: Synchronized fast-frequency oscillations (beta and gamma) are more strictly localized to the contra-lateral somatosensory S1/S2-IC areas[74,79,88,123], whereas slow (delta and theta-alpha) oscillations are mostly expressed at medial fronto-central regions (Figs. 2, 3, 4). Although the precise functional correlates of frequency-specific PROs are currently not clearly understood[10,124], the different dominant engagement of either contra-lateral sensory or associative fronto-medial areas support the view that fast- and slow-frequency PROs contribute differentially to pain processing. Fast-frequency PROs generated within the first 200 ms after noxious events at contra-lateral somatosensory regions as observed here may be more closely linked to the somatosensory discriminative component of pain[89,125], whereas slow-frequency PROs at fronto-medial regions may be more strongly involved in nociceptive integration shaping the cognitive, emotional and motivational components of pain[16,126,127]. It is important to note that the currently analysed spatial synchronization of PROs provides new evidence that distributed oscillatory networks are synchronized at very early stages of pain processing, which may support the early communication of the incoming noxious flow to associative areas. Such spatially synchronized networks may also mediate the influence of the complexity of co-activated cortical and subcortical regions reflecting both bottom-up and top-down mechanisms[2]. Thus, the early inter-regional synchronization may reveal important aspects of the initial communication of pain information, in addition to the secondary translation of this information to distributed brain regions at later stages of pain processing[94].

The main results of the present study provide original evidence that extensive meditation expertise is associated with substantial suppression of PRO synchronization. Specifically, (1) post-stimulus synchronization reduction in LTM was frequency-unspecific as it was observed for multi-spectral oscillations from theta-alpha to gamma ranges; (2) both the temporal and spatial synchronizations were blocked at very early stages (within 200 ms) of pain processing in LTM; (3) pain-related decoupling of post-stimulus oscillations in LTM was observed at the contra-lateral primary and secondary somatosensory regions, and no significant between-group differences were found in fronto-medial regions; and (4) these effects persisted during a non-meditative resting-state. Nickel et al.[89] have reported that pain-related potentials (N1, N2, and P2 components) capturing phase-locked activity and local EEG responses at different frequencies (alpha, beta, and gamma oscillations) are associated with stimulus intensity but not expectations suggesting that the local phase-locked EEG responses are more involved in signalling sensory information than in signalling cognitive/emotional information. Babiloni et al.[74] also have demonstrated that when similar electric stimulation inducing innocuous or noxious perception is applied, the temporal synchronization of theta-to-gamma PROs is significantly enhanced by the high-intensity stimulation. Hence, the early temporal desynchronization of PROs at somatosensory S1 and S2-IC regions implies that sensory bottom-up processes are inhibited in experienced meditators[73]. This is supported by the positive association found here between individual pain threshold and synchronization measures since a higher threshold is linked to greater noxious stimulus intensity. The suppression of spatial synchronization of S1/S2-IC further points to a blocked translation of pain information to higher-order cognitive and emotional evaluation/appraisal regions and may represent a new marker of sensory-cognitive decoupling. The generalized expression of PROs desynchronization in LTM, i.e., the engagement of both the temporal and spatial synchronization and the lack of frequency selectivity, infers that the afferent signalling from ascending pain pathways is overall restricted/filtered in a bottom-up way. Also, as discussed below, the background functional state of the somatosensory cortices may be altered in LTM such that the early processing and communication of noxious input is inhibited at the cortical level. These implications for diminished processing of the sensory pain component contrast the model for nociception in meditation according to which somatosensory areas are over-activated and intensively process the afferent pain input. Instead, they are consistent with the suggestion that meditation is associated with lower signalling in somatosensory areas[73] due to a downregulation of ascending nociceptive signals in the thalamus[64,65,71].

Another major result of the present study is the selective lateralized enhancement of alpha activity in LTM in the contra-lateral hemisphere, which preceded pain stimulus delivery. It is remarkable that although alpha and gamma activities were larger in LTM than STM in both non-meditative no-pain and pain conditions, a

prominent lateralized augmentation of alpha activity in LTM specifically emerged before the painful stimulation. It has been since long widely acknowledged that focusing attention on a relevant or salient stimulus is associated with suppression of spontaneous alpha rhythms at task-relevant cortical regions[128]. This alpha-blocking reflects a preparatory increase in excitability of task-relevant primary sensory (visual, auditory, tactile), motor or associative areas[129,130]. Specifically, for the somatosensory areas, the active role of alpha suppression in attentive preparation has been well documented. Van Ede et al.[92,93] have demonstrated that attentional anticipation of tactile events is characterized by suppression of contralateral alpha (8–12 Hz) and beta (15–30 Hz) oscillations before stimulus, reflecting a brain state in which subsequent neuronal processing efficacy is high. Attention orientation to upcoming painful stimuli also has been verified by the presence of pronounced alpha desynchronization at the contra-lateral primary and secondary somatosensory regions. In a series of studies, Babiloni et al. have demonstrated alpha blocking over the contralateral primary sensorimotor cortex which predicts subsequent subjects' evaluation of pain intensity and intensity discrimination[90,131–134]. In a similar vein, Ploner et al.[84,117] have reported a significant correlation between blocked sensorimotor alpha activity and increased excitability of somatosensory cortices in a pain experiment. Thus, pain expectancy is consistently accompanied by a pre-stimulus blocking of alpha rhythms (rev.[91]) reflecting an automatic attention orientation to upcoming unpleasant and aversive events, a trend also detected here for control subjects.

These previous reports are in striking contrast with the prominent pre-stimulus alpha increase at the contra-lateral S1 and S2-IC observed here in experienced mediators (Fig. 7). While the active role for alpha blocking (event-related desynchronization, ERD) in the mechanisms of attention orientation enjoys robust experimental support, it is now acknowledged that increased alpha activity (event-related synchronization, ERS) represents not only a state of inactivation (idling) but an active general inhibition mechanism across cortical areas[129], through which an organized periodic time structure of the inhibitory processes is provided[129,130,135]. Mathewson et al.[130] specifically propose that the alpha-related cyclic (pulsed) inhibition is efficient only when the power of alpha rhythms is high, thus promoting a generalized synchronization of a multitude of neural populations. In the context of these concepts, the enhanced background alpha activity in LTM in both no-pain and pain conditions points to an overall extended capacity for active cortical inhibition. In addition, the lateralized contra-lateral augmentation of pre-stimulus alpha in LTM before pain stimulation may reflect an active involvement of inhibitory mechanisms to suppress painful input. It is worth noting that in standard (no-pain) experiments in different modalities, alpha enhancements (ERS) have been typically detected as localized asymmetric phenomena at regions which process irrelevant non-target information. Because target-relevant regions manifest a simultaneous alpha suppression (ERD), the augmentation has been regarded as a mechanism supporting a major task by filtering and minimizing irrelevant processing[136–138]. From this perspective, it is especially intriguing that LTM appear not to re-distribute processing resources to optimize ongoing performance. Instead, they appear to be able to deliberately induce a state of inhibition by actively amplifying the alpha rhythms at task-relevant (but not irrelevant) cortical regions, i.e., contra-lateral somatosensory S1 and S2-IC where the painful afferent input is arriving. These results reveal a unique capacity of long-term meditation practitioners to pro-actively control their alpha rhythms. Thus, new evidence is provided for the presence of pro-active top-down inhibition mediated by a controlled guidance of alpha oscillations in meditation. These observations strongly support the model positing a major role of cognitive processes and executive attention for pain regulation in meditation[65,71].

Previous studies have shown that pre-stimulus alpha blocking (ERD) may directly affect subjective pain intensity (e.g.,[90,91]), but no such relations were found here. However, pre-stimulus alpha predicted the suppressed post-stimulus temporal and spatial synchronization of PROs at S1 and S2-IC. Although not derived from single trial analyses[118], this result points to the functional capacity of the large ongoing alpha activity in experienced meditators to block post-stimulus coupling of oscillations and prevent synchronized recruitment of EEG responses, which subsequently modulated pain sensitivity.

Interestingly, the cognitive reappraisal of painful stimuli indexed by P3b was not substantially decreased in LTM as expected by the majority of previous reports[55,57,59–63,68,69]. Existing models also propose a lowered need for pain appraisal in meditation due to sensory-cognitive decoupling or a transformation of the afferent pain input[64]. The non-significant decrease in P3b found in our study suggests that the emotional reflection and cognitive assessment of pain are diminished but not fully abolished in expert meditators. Indeed, subjective pain measures (intensity perception, aversion, identification) were decreased in LTM but did not differ significantly between the groups in the non-meditative resting state, as also reported by others[39,66,67]. Importantly, however, the lack of significant alteration of synchronized fronto-medial oscillations and P3b points to a critical dissociation between a pro-active (inhibitory) and reactive top-down mechanisms of pain processing that appear to be separately employed by long-term meditators. Such a dissociation may explain the capacity of LTM to inhibit or down-regulate the processing and neural transmission of expected negative influences, while preserving a sufficiently strong attentional focus and awareness after each external event.

Taken together, the present analyses of pain-related oscillations reveal new neurophysiologic mechanisms of pain processing in meditation. They show that even in non-meditative pain conditions, experienced meditators exhibit a top-down pro-active inhibition of somatosensory areas through deliberately controlling brain alpha rhythms. As a result, the temporal and spatial synchronization of their pain-related neural responses is compromised leading to suppressed processing and communication of sensory pain information at early stages of painful input. Although the translation of sensory information is suppressed suggesting sensory-cognitive uncoupling, the subsequent reactive emotional/cognitive evaluation of pain remains preserved. These findings provide new insights into the neural mechanisms of top-down pain control and in particular, the effects of meditation practice on these mechanisms.

Expressed in terms of the Buddhist psychological model of the two arrows of pain, our results provide general support for its claim that two significant stages of pain processing can be distinguished[139]. According to this view, the first arrow of pain represents the 'bodily' or somatosensory stage while the second arrow represents

the 'mental' stage, the evaluative, cognitive-affective component of pain processing (also see[58]). Our data suggest that extensive meditation practice reduces pain by suppressing the first arrow of pain and also by suppressing its propagation towards the second arrow.

Data availability

The datasets used and analysed during the current study are available from the corresponding author on reasonable request.

Received: 30 December 2024; Accepted: 12 March 2025
Published online: 27 March 2025

References

1. Bushnell, M. C., Ceko, M. & Low, L. A. Cognitive and emotional control of pain and its disruption in chronic pain. *Nat. Rev. Neurosci.* **14**, 502–511. https://doi.org/10.1038/nrn3516 (2013).
2. Chen, Z. S. Hierarchical predictive coding in distributed pain circuits. *Front. Neural Circuits* **17**, 1073537. https://doi.org/10.3389/fncir.2023.1073537 (2023).
3. Moayedi, M. & Davis, K. D. Theories of pain: from specificity to gate control. *J. Neurophysiol.* **109**, 5–12. https://doi.org/10.1152/jn.00457.2012 (2013).
4. Price, D. D. Psychological and neural mechanisms of the affective dimension of pain. *Science* **288**, 1769–1772. https://doi.org/10.1126/science.288.5472.1769 (2000).
5. Rainville, P. Brain mechanisms of pain affect and pain modulation. *Curr. Opin. Neurobiol.* **12**, 195–204. https://doi.org/10.1016/s0959-4388(02)00313-6 (2002).
6. Seminowicz, D. A. & Davis, K. D. A re-examination of pain cognition interactions: implications for neuroimaging. *PAIN* **130**, 8–13. https://doi.org/10.1016/j.pain.2007.03.036 (2007).
7. Apkarian, A. V., Bushnell, M. C., Treede, R. D. & Zubieta, J. K. Human brain mechanisms of pain perception and regulation in health and disease. *Eur. J. Pain* **9**, 463–484. https://doi.org/10.1016/j.ejpain.2004.11.001 (2005).
8. Kucyi, A. & Davis, K. D. The dynamic pain connectome. *Trends Neurosci.* **38**, 86–95. https://doi.org/10.1016/j.tins.2014.11.006 (2015).
9. Wiech, K. Deconstructing the sensation of pain: The influence of cognitive processes on pain perception. *Science* **354**, 584–587. https://doi.org/10.1126/science.aaf8934 (2016).
10. Ploner, M., Sorg, C. & Gross, J. Brain rhythms of pain. *Trends Cogn. Sci.* **21**, 100–110. https://doi.org/10.1016/j.tics.2016.12.001 (2017).
11. Wiech, K., Ploner, M. & Tracey, I. Neurocognitive aspects of pain perception. *Trends Cogn. Sci.* **12**, 306–313. https://doi.org/10.1016/j.tics.2008.05.005 (2008).
12. Garcia-Larrea, L. & Peyron, R. Pain matrices and neuropathic pain matrices: a review. *PAIN* **154**, S29–S43. https://doi.org/10.1016/j.pain.2013.09.001 (2013).
13. Iannetti, G. D. & Mouraux, A. From the neuromatrix to the pain matrix (and back). *Exp. Brain. Res.* **205**, 1–12. https://doi.org/10.1007/s00221-010-2340-1 (2010).
14. Kucyi, A. & Davis, K. D. The neural code for pain: From single-cell electrophysiology to the dynamic pain connectome. *Neuroscientist* **23**, 397–414. https://doi.org/10.1177/1073858416667716 (2017).
15. Mano, H. & Seymour, B. Pain: a distributed brain information network?. *PLoS Biol* **13**, e1002037. https://doi.org/10.1371/journal.pbio.1002037 (2015).
16. Peyron, R., Laurent, B. & Garcia-Larrea, L. Functional imaging of brain responses to pain. *A Rev. meta-analysis. Neurophysiol. Clin.* **30**, 263–288. https://doi.org/10.1016/s0987-7053(00)00227-6 (2000).
17. Davis, K. D. & Moayedi, M. Central mechanisms of pain revealed through functional and structural MRI. *J. Neuroimmune Pharmacol.* **8**, 518–534. https://doi.org/10.1007/s11481-012-9386-8 (2013).
18. Garcia-Larrea, L., Frot, M. & Valeriani, M. Brain generators of laser-evoked potentials: from dipoles to functional significance. *Neurophysiol. Clin.* **33**, 279–292. https://doi.org/10.1016/j.neucli.2003.10.008 (2003).
19. Ma, Q. A functional subdivision within the somatosensory system and its implications for pain research. *Neuron* **110**, 749–769. https://doi.org/10.1016/j.neuron.2021.12.015 (2022).
20. Peyron, R. et al. Haemodynamic brain responses to acute pain in humans: sensory and attentional networks. *Brain* **122**, 1765–1779. https://doi.org/10.1093/brain/122.9.1765 (1999).
21. Wager, T. D. et al. Pain in the ACC?. *Proc. Natl. Acad. Sci. USA* **113**, E2474-2475. https://doi.org/10.1073/pnas.1600282113 (2016).
22. Willis, W. D. & Westlund, K. N. Neuroanatomy of the pain system and of the pathways that modulate pain. *J. Clin. Neurophysiol.* **14**, 2–31. https://doi.org/10.1097/00004691-199701000-00002 (1997).
23. Fiorio, M. et al. Enhancing non-noxious perception: behavioural and neurophysiological correlates of a placebo-like manipulation. *Neuroscience* **217**, 96–104. https://doi.org/10.1016/j.neuroscience.2012.04.066 (2012).
24. Iannetti, G. D., Hughes, N. P., Lee, M. C. & Mouraux, A. Determinants of laser-evoked EEG responses: pain perception or stimulus saliency?. *J. Neurophysiol.* **100**, 815–828. https://doi.org/10.1152/jn.00097.2008 (2008).
25. Liberati, G. et al. Habituation of phase-locked local field potentials and gamma-band oscillations recorded from the human insula. *Sci. Rep.* **8**, 8265. https://doi.org/10.1038/s41598-018-26604-0 (2018).
26. Niso, G., Tjepkema-Cloostermans, M. C., Lenders, M. W. P. M. & de Vos, C. C. Modulation of the somatosensory evoked potential by attention and spinal cord stimulation. *Front. Neurol.* **12**, 694310. https://doi.org/10.3389/fneur.2021.694310 (2021).
27. Zhang, Z. G., Hu, L., Hung, Y. S., Mouraux, A. & Iannetti, G. D. Gamma-band oscillations in the primary somatosensory cortex - a direct and obligatory correlate of subjective pain intensity. *J. Neurosci.* **32**, 7429–7438. https://doi.org/10.1523/JNEUROSCI.5877-11.2012 (2012).
28. Atlas, L. Y. How instructions, learning, and expectations shape pain and neurobiological responses. *Ann. Rev. Neurosci.* **46**, 167–189. https://doi.org/10.1146/annurev-neuro-101822-122427 (2023).
29. Peerdeman, K. J. et al. Relieving patients' pain with expectation interventions: a meta-analysis. *PAIN* **157**, 1179–1191. https://doi.org/10.1097/j.pain.0000000000000540 (2016).
30. Cheng, J. C., Erpelding, N., Kucyi, A., DeSouza, D. D. & Davis, K. D. Individual differences in temporal summation of pain reflect pronociceptive and antinociceptive brain structure and function. *J. Neurosci.* **35**, 9689–9700. https://doi.org/10.1523/jneurosci.5039-14.2015 (2015).
31. Mussigmann, T., Bardel, B. & Lefaucheur, J. P. Resting-state electroencephalography (EEG) biomarkers of chronic neuropathic pain. *A Systematic Rev. NeuroImage* **258**, 119351. https://doi.org/10.1016/j.neuroimage.2022.119351 (2022).
32. Napadow, V., Kim, J., Clauw, D. J. & Harris, R. E. Decreased intrinsic brain connectivity is associated with reduced clinical pain in fibromyalgia. *Arthritis Rheum* **64**, 2398–2403. https://doi.org/10.1002/art.34412 (2012).
33. Pfannmöller, J. & Lotze, M. Review on biomarkers in the resting-state networks of chronic pain patients. *Brain Cogn* **131**, 4–9. https://doi.org/10.1016/j.bandc.2018.06.005 (2019).

34. Spisak, T. et al. Pain-free resting-state functional brain connectivity predicts individual pain sensitivity. *Nat. Commun.* **11**, 187. https://doi.org/10.1038/s41467-019-13785-z (2020).
35. Ta Dinh S, Nickel MM, Tiemann L, May ES, Heitmann H, Hohn VD, Edenharter G, Utpadel-Fischler D, Tölle TR, Sauseng P, Gross J, Ploner M. Brain dysfunction in chronic pain patients assessed by resting-state electroencephalography. PAIN 2019;160:2751–2765. https://doi.org/10.1097/j.pain.0000000000001666 Erratum in: PAIN;161:1684. https://doi.org/10.1097/j.pain.0000000000001948 (2020).
36. Tu, Y. et al. Identifying inter-individual differences in pain threshold using brain connectome: a test-retest reproducible study. *NeuroImage* **202**, 116049. https://doi.org/10.1016/j.neuroimage.2019.116049 (2019).
37. Cahn, B. R. & Polich, J. Meditation states and traits: EEG, ERP, and neuroimaging studies. *Psychol. Bull.* **132**, 180–211. https://doi.org/10.1037/0033-2909.132.2.180 (2006).
38. Isbel, B. & Summers, M. J. Distinguishing the cognitive processes of mindfulness: Developing a standardised mindfulness technique for use in longitudinal randomised control trials. *Consc. Cogn.* **52**, 75–92. https://doi.org/10.1016/j.concog.2017.04.019 (2017).
39. Lutz, A., Slagter, H. A., Dunne, J. D. & Davidson, R. J. Attention regulation and monitoring in meditation. *Trends Cogn. Sci.* **12**, 163–169. https://doi.org/10.1016/j.tics.2008.01.005 (2008).
40. Malinowski, P. Neural mechanisms of attentional control in mindfulness meditation. *Front. Neurosci.* **7**, 8. https://doi.org/10.3389/fnins.2013.00008 (2013).
41. Raffone A, Srinivasan N, Barendregt HP. Attention, consciousness and mindfulness in meditation. Psychology of Meditation. USA: Nova Science Publishers, 2014, pp. 147–66.
42. Raffone, A. et al. Toward a brain theory of meditation. *Progr. Brain Res.* **244**, 207–232. https://doi.org/10.1016/bs.pbr.2018.10.028 (2019).
43. Vago, D. R. & Silbersweig, D. A. Self-awareness, self-regulation, and self-transcendence (S-ART): a framework for understanding the neurobiological mechanisms of mindfulness. *Front. Hum. Neurosci.* **6**, 296. https://doi.org/10.3389/fnhum.2012.00296 (2012).
44. Hölzel, B. K. et al. Mindfulness practice leads to increases in regional brain gray matter density. *Psychiatry Res. Neuroimaging* **191**, 36–43. https://doi.org/10.1016/j.pscychresns.2010.08.006 (2011).
45. Jensen, M. P., Day, M. A. & Miró, J. Neuromodulatory treatments for chronic pain: efficacy and mechanisms. *Nat. Rev. Neurol.* **10**, 167–178. https://doi.org/10.1038/nrneurol.2014.12 (2014).
46. Su, I. W. et al. Pain perception can be modulated by mindfulness training: a resting-state fMRI study. *Front. Hum. Neurosci.* **10**, 570. https://doi.org/10.3389/fnhum.2016.00570 (2016).
47. Yordanova, J. et al. Common and distinct lateralised patterns of neural coupling during focused attention, open monitoring and loving kindness meditation. *Sci. Rep.* **10**, 7430. https://doi.org/10.1038/s41598-020-64324-6 (2020).
48. Manna, A. et al. Neural correlates of focused attention and cognitive monitoring in meditation. *Brain Res. Bull.* **82**, 46–56. https://doi.org/10.1016/j.brainresbull.2010.03.001 (2010).
49. Sezer, I., Pizzagalli, D. A. & Sacchet, M. D. Resting-state fMRI functional connectivity and mindfulness in clinical and non-clinical contexts: a review and synthesis. *Neurosci. Biobehav. Rev.* **135**, 104583. https://doi.org/10.1016/j.neubiorev.2022.104583 (2022).
50. Yordanova, J. et al. Attentional and cognitive monitoring brain networks in long-term meditators depend on meditation states and expertise. *Sci. Rep.* **11**, 4909. https://doi.org/10.1038/s41598-021-84325-3 (2021).
51. Guidotti, R. et al. Long-term and meditation-specific modulations of brain connectivity revealed through multivariate pattern analysis. *Brain Topogr.* **36**, 409–418. https://doi.org/10.1007/s10548-023-00950-3 (2023).
52. Fox, K. C. R. et al. Is meditation associated with altered brain structure? A systematic review and meta-analysis of morphometric neuroimaging in meditation practitioners. *Neurosci. Biobehav. Rev.* **43**, 48–73. https://doi.org/10.1016/j.neubiorev.2014.03.016 (2014).
53. Lu, C., Moliadze, V. & Nees, F. Dynamic processes of mindfulness-based alterations in pain perception. *Front. Neurosci.* **17**, 1253559. https://doi.org/10.3389/fnins.2023.1253559 (2023).
54. Tang, Y. Y., Hölzel, B. K. & Posner, M. I. The neuroscience of mindfulness meditation. *Nat. Rev. Neurosci.* **16**, 213–225. https://doi.org/10.1038/nrn3916 (2015).
55. Bakhshani, N. M., Amirani, A., Amirifard, H. & Shahrakipoor, M. The effectiveness of mindfulness-based stress reduction on perceived pain intensity and quality of life in patients with chronic headache. *Global J. Health Sci.* **8**, 47326. https://doi.org/10.5539/gjhs.v8n4p142 (2016).
56. Grant, J. A. & Rainville, P. Pain sensitivity and analgesic effects of mindful states in Zen meditators: a cross-sectional study. *Psychosom. Med.* **71**, 106–114. https://doi.org/10.1097/psy.0b013e31818f52ee (2009).
57. Grossman, P., Tiefenthaler-Gilmer, U., Raysz, A. & Kesper, U. Mindfulness training as an intervention for fibromyalgia: evidence of postintervention and 3-year follow-up benefits in well-being. *Psychother Psychosom* **76**, 226. https://doi.org/10.1159/000101501 (2007).
58. Nicolardi, V. et al. The two arrows of pain: mechanisms of pain related to meditation and mental states of aversion and identification. *Mindfulness* **15**, 753–774. https://doi.org/10.1007/s12671-021-01797-0 (2022).
59. Schmidt, S. et al. Treating fibromyalgia with mindfulness-based stress reduction: results from a 3-armed randomized controlled trial. *PAIN* **152**, 361–369. https://doi.org/10.1016/j.pain.2010.10.043 (2011).
60. Brefczynski-Lewis, J. A., Lutz, A., Schaefer, H. S., Levinson, D. B. & Davidson, R. J. Neural correlates of attentional expertise in long-term meditation practitioners. *Proc. Natl. Acad. Sci. USA* **104**, 11483–11488. https://doi.org/10.1073/pnas.0606552104 (2007).
61. Kasai, Y. et al. Psychological effects of meditation at a Buddhist monastery in Myanmar. *J. Mental Health* **26**, 4–7. https://doi.org/10.3109/09638237.2015.1124405 (2017).
62. Morone, N. E., Greco, C. M. & Weiner, D. K. Mindfulness meditation for the treatment of chronic low back pain in older adults: a randomized controlled pilot study. *PAIN* **134**, 310–319. https://doi.org/10.1016/j.pain.2007.04.038 (2008).
63. Nielsen, L. & Kaszniak, A. W. Awareness of subtle emotional feelings: a comparison of long-term meditators and nonmeditators. *Emotion* **6**, 392–405. https://doi.org/10.1037/1528-3542.6.3.392Erratum.In:Emotion2007;7:754 (2006).
64. Jinich-Diamant, A. et al. Neurophysiological mechanisms supporting mindfulness meditation-based pain relief: an updated review. *Curr. Pain Headache Rep.* **24**, 56. https://doi.org/10.1007/s11916-020-00890-8 (2020).
65. Zeidan, F. & Vago, D. R. Mindfulness meditation–based pain relief: a mechanistic account. *Ann. NY. Acad. Sci.* **1373**, 114–127. https://doi.org/10.1111/NYAS.13153 (2016).
66. Gard, T. et al. Pain attenuation through mindfulness is associated with decreased cognitive control and increased sensory processing in the brain. *Cereb Cortex* **22**, 2692–2702. https://doi.org/10.1093/cercor/bhr352 (2011).
67. Grant, J. A., Courtemanche, J. & Rainville, P. A non-elaborative mental stance and decoupling of executive and pain-related cortices predicts low pain sensitivity in Zen meditators. *PAIN* **152**, 150–156. https://doi.org/10.1016/j.pain.2010.10.006 (2011).
68. Zorn, J., Abdoun, O., Bouet, R. & Lutz, A. Mindfulness meditation is related to sensory-affective uncoupling of pain in trained novice and expert practitioners. *Eur. J. Pain* **24**, 1301–1313. https://doi.org/10.1002/ejp.1576 (2020).
69. Zorn, J., Abdoun, O., Sonié, S. & Lutz, A. Cognitive defusion is a core cognitive mechanism for the sensory-affective uncoupling of pain during mindfulness meditation. *Psychosom Med.* **83**, 566–578. https://doi.org/10.1097/PSY.0000000000000938 (2021).
70. Perlman, D. M., Salomons, T. V., Davidson, R. J. & Lutz, A. Differential effects on pain intensity and unpleasantness of two meditation practices. *Emotion* **10**, 65. https://doi.org/10.1037/a0018440 (2010).

71. Zeidan, F. et al. Brain mechanisms supporting the modulation of pain by mindfulness meditation. *J. Neurosci.* **31**, 5540–5548. https://doi.org/10.1523/JNEUROSCI.5791-10.2011 (2011).
72. Zeidan, F. et al. Mindfulness meditation-based pain relief employs different neural mechanisms than placebo and sham mindfulness meditation-induced analgesia. *J. Neurosci.* **35**, 15307–15325. https://doi.org/10.1523/jneurosci.2542-15.2015 (2015).
73. Brown, C. A. & Jones, A. K. Meditation experience predicts less negative appraisal of pain: Electrophysiological evidence for the involvement of anticipatory neural responses. *PAIN* **150**, 428–438. https://doi.org/10.1016/j.pain.2010.04.017 (2010).
74. Babiloni, C. et al. Human brain oscillatory activity phase-locked to painful electrical stimulations: a multi-channel EEG study. *Hum. Brain Map.* **15**, 112–123. https://doi.org/10.1002/hbm.10013 (2002).
75. Gross, J., Schnitzler, A., Timmermann, L. & Ploner, M. Gamma oscillations in human primary somatosensory cortex reflect pain perception. *PLOS Biol* **5**, e133. https://doi.org/10.1371/journal.pbio.0050133 (2007).
76. Hauck, M., Lorenz, J. & Engel, A. K. Attention to painful stimulation enhances gamma-band activity and synchronization in human sensorimotor cortex. *J. Neurosci.* **27**, 9270–9277. https://doi.org/10.1523/jneurosci.2283-07.2007 (2007).
77. Hauck, M., Domnick, C., Lorenz, J., Gerloff, C. & Engel, A. K. Top-down and bottom-up modulation of pain induced oscillations. *Front. Hum. Neurosci.* **9**, 375. https://doi.org/10.3389/fnhum.2015.00375 (2015).
78. Hu, L., Peng, W., Valentini, E., Zhang, Z. & Hu, Y. Functional features of nociceptive-induced suppression of alpha band electroencephalographic oscillations. *J. Pain.* **14**, 89–99. https://doi.org/10.1016/j.jpain.2012.10.008 (2013).
79. Liu, C. C. et al. Functional role of induced gamma oscillatory responses in processing noxious and innocuous sensory events in humans. *Neuroscience* **310**, 389–400. https://doi.org/10.1016/j.neuroscience.2015.09.047 (2015).
80. Lorenz, J. & Garcia-Larrea, L. Contribution of attentional and cognitive factors to laser evoked brain potentials. *Neurophysiol. Clin.* **33**, 293–301. https://doi.org/10.1016/j.neucli.2003.10.004 (2003).
81. May, E. S. et al. Pre- and post-stimulus alpha activity shows differential modulation with spatial attention during the processing of pain. *NeuroImage* **62**, 1965–1974. https://doi.org/10.1016/j.neuroimage.2012.05.071 (2012).
82. Mouraux, A., Guérit, J. M. & Plaghki, L. Non-phase locked electroencephalogram (EEG) responses to CO2 laser skin stimulations may reflect central interactions between A partial partial differential- and C-fibre afferent volleys. *Clin. Neurophysiol.* **114**, 710–722. https://doi.org/10.1016/s1388-2457(03)00027-0 (2003).
83. Northon, S., Deldar, Z. & Piché, M. Spinal and cerebral integration of noxious inputs in left-handed individuals. *Brain Topogr.* **34**, 568–586. https://doi.org/10.1007/s10548-021-00864-y (2021).
84. Ploner, M., Gross, J., Timmermann, L., Pollok, B. & Schnitzler, A. Pain suppresses spontaneous brain rhythms. *Cereb Cortex* **16**, 537–540. https://doi.org/10.1093/cercor/bhj001 (2006).
85. Strube, A., Rose, M., Fazeli, S. & Buchel, C. Spatial and spectral characteristics of expectations and prediction errors in pain and thermoception. *eLife* https://doi.org/10.7554/eLife.62809 (2021).
86. Tiemann, L., Schulz, E., Gross, J. & Ploner, M. Gamma oscillations as a neuronal correlate of the attentional effects of pain. *PAIN* **150**, 302–308. https://doi.org/10.1016/j.pain.2010.05.014 (2010).
87. Tiemann, L. et al. Differential neurophysiological correlates of bottom-up and top-down modulations of pain. *PAIN* **156**, 289–296. https://doi.org/10.1097/01.j.pain.0000460309.94442.44 (2015).
88. Yue, L., Iannetti, G. D. & Hu, L. The neural origin of nociceptive-induced gamma-band oscillations. *J. Neurosci.* **40**, 3478–3490. https://doi.org/10.1523/JNEUROSCI.0255-20.2020 (2020).
89. Nickel, M. M. et al. Temporal-spectral signaling of sensory information and expectations in the cerebral processing of pain. *Proc. Natl. Acad. Sci. USA* **119**, e2116616119. https://doi.org/10.1073/pnas.2116616119 (2022).
90. Babiloni, C. et al. Anticipatory electroencephalography alpha rhythm predicts subjective perception of pain intensity. *J. Pain* **7**, 709–717. https://doi.org/10.1016/j.jpain.2006.03.005 (2006).
91. Peng, W., Babiloni, C., Mao, Y. & Hu, Y. Subjective pain perception mediated by alpha rhythms. *Biol Psychol* **109**, 141–150. https://doi.org/10.1016/j.biopsycho.2015.05.004 (2015).
92. van Ede, F., Jensen, O. & Maris, E. Tactile expectation modulates pre-stimulus beta-band oscillations in human sensorimotor cortex. *NeuroImage* **51**, 867–876. https://doi.org/10.1016/j.neuroimage.2010.02.053 (2010).
93. van Ede, F., de Lange, F., Jensen, O. & Maris, E. Orienting attention to an upcoming tactile event involves a spatially and temporally specific modulation of sensorimotor alpha- and beta-band oscillations. *J. Neurosci.* **31**, 2016–2024. https://doi.org/10.1523/JNEUROSCI.5630-10.2011 (2011).
94. Bott, F. S. et al. Local brain oscillations and interregional connectivity differentially serve sensory and expectation effects on pain. *Sci. Adv.* https://doi.org/10.1126/sciadv.add7572 (2023).
95. Polich, J. Updating P300: an integrative theory of P3a and P3b. *Clin. Neurophysiol.* **118**, 2128–2148. https://doi.org/10.1016/j.clinph.2007.04.019 (2007).
96. Legrain, V., Guérit, J. M., Bruyer, R. & Plaghki, L. Attentional modulation of the nociceptive processing into the human brain: selective spatial attention, probability of stimulus occurrence, and target detection effects on laser evoked potentials. *PAIN* **99**, 21–39. https://doi.org/10.1016/s0304-3959(02)00051-9 (2002).
97. Legrain, V. et al. A neurocognitive model of attention to pain: behavioral and neuroimaging evidence. *PAIN* **144**, 230–232. https://doi.org/10.1016/j.pain.2009.03.020 (2009).
98. Legrain, V. et al. Cognitive aspects of nociception and pain: bridging neurophysiology with cognitive psychology. *Neurophysiol. Clin.* **42**, 325–336. https://doi.org/10.1016/j.neucli.2012.06.003 (2012).
99. Säterö, P., Klingenstierna, U., Karlsson, T. & Olausson, B. Pain threshold measurements with cutaneous argon laser, comparing a forced choice and a method of limits. *Prog. Neuropsychopharmacol. Biol. Psychiatry* **24**, 397–407. https://doi.org/10.1016/s0278-5846(99)00107-4 (2000).
100. Valentini, E., Nicolardi, V. & Aglioti, S. M. Painful engrams: Oscillatory correlates of working memory for phasic nociceptive laser stimuli. *Brain Cogn.* **115**, 21–32. https://doi.org/10.1016/j.bandc.2017.03.009 (2017).
101. Perrin, F., Pernier, J., Bertrand, O. & Echallier, J. F. Spherical splines for scalp potential and current density mapping. *Electroencephalogr. Clin. Neurophysiol.* **72**, 184–187. https://doi.org/10.1016/0013-4694(89)90180-6 (1989).
102. Makeig, S., Bell, A. J., Jung, T.-P., Ghahremani, D. & Sejnowski, T. J. Blind separation of auditory event-related brain responses into independent components. *Proc. Natl. Acad. Sci. USA* **94**, 10979–10984. https://doi.org/10.1073/pnas.94.20.10979 (1997).
103. Nunez, P. L. et al. EEG coherency. I: Statistics reference electrode volume conduction Laplacians cortical imaging and interpretation at multiple scales. *Electroencephalogr. Clin. Neurophysiol.* **103**, 499–515. https://doi.org/10.1016/s0013-4694(97)00066-7 (1997).
104. Başar, E., Başar-Eroglu, C., Karakaş, S. & Schürmann, M. Gamma, alpha, delta, and theta oscillations govern cognitive processes. *Int. J. Psychophysiol.* **39**, 241–248. https://doi.org/10.1016/s0167-8760(00)00145-8 (2001).
105. Kolev, V., Falkenstein, M. & Yordanova, J. Aging and error processing: Time-frequency analysis of error-related potentials. *J. Psychophysiol.* **19**, 289–297. https://doi.org/10.1027/0269-8803.19.4.289ISSN0269-8803 (2005).
106. Kolev, V., Falkenstein, M. & Yordanova, J. A distributed theta network of error generation and processing in aging. *Cogn. Neurodyn.* **18**, 447–459. https://doi.org/10.1007/s11571-023-10018-4 (2024).
107. Yordanova, J. & Kolev, V. Single-sweep analysis of the theta frequency band during an auditory oddball task. *Psychophysiology* **35**, 116–126. https://doi.org/10.1111/1469-8986.3510116 (1998).
108. Mallat, S. *A Wavelet Tour of Signal Processing, 2nd edR* (Academic Press, 1999).
109. Yordanova, J., Falkenstein, M. & Kolev, V. Aging-related changes in motor response-related theta activity. *Int. J Psychophysiol.* **153**, 95–106. https://doi.org/10.1016/j.ijpsycho.2020.03.005 (2020).

110. Lachaux, J. P., Rodriguez, E., Martinerie, J. & Varela, F. J. Measuring phase synchrony in brain signals. *Hum. Brain Map.* **8**, 194–208 (1999).
111. Tallon-Baudry, C., Bertrand, O., Delpuech, C. & Permier, J. Oscillatory gamma-band (30–70 Hz) activity induced by a visual search task in humans. *J. Neurosci.* **17**, 722–734. https://doi.org/10.1523/JNEUROSCI.17-02-00722.1997 (1997).
112. Cohen, M. X. *Analyzing neural time series data: Theory and practice* (The MIT Press, 2014).
113. Koessler, L. et al. Automatic localization and labeling of EEG sensors (ALLES) in MRI volume. *NeuroImage* **41**, 914–923. https://doi.org/10.1016/j.neuroimage.2008.02.039 (2008).
114. Scrivener, C. L. & Reader, A. T. Variability of EEG electrode positions and their underlying brain regions: visualizing gel artifacts from a simultaneous EEG-fMRI dataset. *Brain Behav.* **12**, e2476. https://doi.org/10.1002/brb3.2476 (2022).
115. Benjamini, Y. & HochbergY.,. Controlling the false discovery rate: a practical and powerful approach to multiple testing. *R Stat Soc. B.* **57**, 289–300 (1995).
116. Fell, J., Axmacher, N. & Haupt, S. From alpha to gamma: electrophysiological correlates of meditation-related states of consciousness. *Med. Hypotheses.* **75**, 218–224. https://doi.org/10.1016/j.mehy.2010.02.025 (2010).
117. Ploner, M., Gross, J., Timmermann, L., Pollok, B. & Schnitzler, A. Oscillatory activity reflects the excitability of the human somatosensory system. *NeuroImage* **32**, 1231–1236. https://doi.org/10.1016/j.neuroimage.2006.06.004 (2006).
118. Kolev, V. & Schürmann, M. Event-related prolongation of induced EEG rhythmicities in experiments with a cognitive task. *Int. J. Neurosci.* **67**, 199–213. https://doi.org/10.3109/00207459208994785 (1992).
119. Allison, T., McCarthy, G., Wood, C. C. & Jones, S. J. Potentials evoked in human and monkey cerebral cortex by stimulation of the median nerve. A review of scalp and intracranial recordings. *Brain.* **114**, 2465–2503. https://doi.org/10.1093/brain/114.6.2465 (1991).
120. Chen, L. et al. Pain Vision-based evaluation of brain potentials: a novel approach for quantitative pain assessment. *Front. Bioeng. Biotechnol.* **11**, 1197070. https://doi.org/10.3389/fbioe.2023.1197070 (2023).
121. Peng, W. & Tang, D. Pain related cortical oscillations: Methodological advances and potential applications. *Front. Comput. Neurosci.* **10**, 9. https://doi.org/10.3389/fncom.2016.00009 (2016).
122. Arnfred, S. M., Hansen, L. K., Parnas, J. & Mørup, M. Proprioceptive evoked gamma oscillations. *Brain Res.* **1147**, 167–174. https://doi.org/10.1016/j.brainres.2007.02.068 (2007).
123. Senkowski, D., Kautz, J., Hauck, M., Zimmermann, R. & Engel, A. K. Emotional facial expressions modulate pain-induced beta and gamma oscillations in sensorimotor cortex. *J. Neurosci.* **31**, 14542–14550. https://doi.org/10.1523/JNEUROSCI.6002-10.2011 (2011).
124. Mouraux, A. & Iannetti, G. D. The search for pain biomarkers in the human brain. *Brain* **141**, 3290–3307. https://doi.org/10.1093/brain/awy281 (2018).
125. Hagiwara, K. et al. Oscillatory gamma synchronization binds the primary and secondary somatosensory areas in humans. *NeuroImage* **51**, 412–420. https://doi.org/10.1016/j.neuroimage.2010.02.001 (2010).
126. Dockstader, C., Cheyne, D. & Tannock, R. Cortical dynamics of selective attention to somatosensory events. *NeuroImage* **49**, 1777–1785. https://doi.org/10.1016/j.neuroimage.2009.09.035 (2010).
127. Kenefati, G. et al. Changes in alpha, theta, and gamma oscillations in distinct cortical areas are associated with altered acute pain responses in chronic low back pain patients. *Front. Neurosci.* **17**, 1278183. https://doi.org/10.3389/fnins.2023.1278183 (2023).
128. Pfurtscheller, G. & Lopes da Silva, F. H. Event-related EEG/MEG synchronization and desynchronization: basic principles. *Clin. Neurophysiol.* **110**, 1842–1857. https://doi.org/10.1016/s1388-2457(99)00141-8 (1999).
129. Klimesch, W., Sauseng, P. & Hanslmayr, S. EEG alpha oscillations: the inhibition-timing hypothesis. *Brain Res. Rev.* **53**, 63–88. https://doi.org/10.1016/j.brainresrev.2006.06.003 (2007).
130. Mathewson, K. E. et al. Pulsed out of awareness: EEG alpha oscillations represent a pulsed-inhibition of ongoing cortical processing. *Front. Psychol.* **2**, 99. https://doi.org/10.3389/fpsyg.2011.00099 (2011).
131. Babiloni, C. et al. Anticipatory cortical responses during the expectancy of a predictable painful stimulation A high-resolution electroencephalography study. *Eur. J. Neurosci.* **18**, 1692–1700. https://doi.org/10.1046/j.1460-9568.2003.02851.x (2003).
132. Babiloni, C. et al. Attentional processes and cognitive performance during expectancy of painful galvanic stimulations: a high-resolution EEG study. *Behav. Brain Res.* **152**, 137–147. https://doi.org/10.1016/j.bbr.2003.10.004 (2004).
133. Babiloni, C. et al. Cortical alpha rhythms are related to the anticipation of sensorimotor interaction between painful stimuli and movements: a high-resolution EEG study. *J. Pain* **9**, 902–911. https://doi.org/10.1016/j.jpain.2008.05.007 (2008).
134. Babiloni, C. et al. Pre-stimulus alpha power affects vertex N2–P2 potentials evoked by noxious stimuli. *Brain Res. Bull.* **75**, 581–590. https://doi.org/10.1016/j.brainresbull.2007.09.009 (2008).
135. Jensen, O. & Mazaheri, A. Shaping functional architecture by oscillatory alpha activity: gating by inhibition. *Front. Hum. Neurosci.* **4**, 186. https://doi.org/10.3389/fnhum.2010.00186 (2010).
136. Sauseng, P. et al. A shift of visual spatial attention is selectively associated with human EEG alpha activity. *Neuroscience* **22**, 2917–2926. https://doi.org/10.1111/j.1460-9568.2005.04482.x (2005).
137. Thut, G., Nietzel, A., Brandt, S. A. & Pascual-Leone, A. Alpha-band electroencephalographic activity over occipital cortex indexes visuospatial attention bias and predicts visual target detection. *J. Neurosci.* **26**, 9494–9502. https://doi.org/10.1523/jneurosci.0875-06.20061093/cercor/bhj001 (2006).
138. Worden, M. S., Foxe, J. J., Wang, N. & Simpson, G. V. Anticipatory biasing of visuospatial attention indexed by retinotopically specific alpha-band electroencephalography increases over occipital cortex. *J. Neurosci.* **20**, 63. https://doi.org/10.1523/jneurosci.20-06-j0002.2000 (2000).
139. Nyanaponika Thera. *Sallatha Sutta: The Dart* (translated from the Pali). Buddhist Publication Society, 1998.

Acknowledgements

We would like to express our gratitude and appreciation to the monks, nuns and novices of Amaravati and Santacittarama Buddhist Monasteries for their outstanding dedication and participation in our study. This work has been supported by a grant from BIAL Foundation (Portugal) for the project "Advancements on the aware mind-brain: New insights about the neural correlates of meditation states and traits" (Grant 272/70), and by the National Research Fund by the Ministry of Education and Science, Sofia, Bulgaria (Project KP-06-N33/11/2019).

Author contributions

J.Y., V.N., A.R., and S.M.A. designed the study; L.S. prepared part of the software for data acquisition; V.N., L.S., and A.R acquired the data; J.Y. and V.K. processed and analyzed the data, and prepared the figures; J.Y., S.M.A., and A.R. interpreted the data; J.Y., V.K., A.R. and P.M. wrote the main manuscript text.

Funding

Bulgarian National Science Fund, KP-06-N33/11, KP-06-N33/11, Fundação Bial.

Declarations

Competing interests
The authors declare no competing interests.

Additional information
Correspondence and requests for materials should be addressed to J.Y.

Reprints and permissions information is available at www.nature.com/reprints.

Publisher's note Springer Nature remains neutral with regard to jurisdictional claims in published maps and institutional affiliations.